



Cite this: *Mater. Adv.*, 2022,  
3, 3101

## Prospects of nano-carbons as emerging catalysts for enzyme-mimetic applications

Nisha Dhiman,<sup>a</sup> Somnath Ghosh,<sup>a</sup> Yogendra Kumar Mishra<sup>id</sup><sup>b</sup> and Kumud Malika Tripathi<sup>id</sup><sup>\*a</sup>

It is of enormous scientific and practical significance to develop nanozymes, *i.e.*, enzyme-mimicking nanomaterials, to overcome the instability, difficult storage, and high cost of natural enzymes. The field of enzyme mimetics has advanced significantly after the emergence of nano-carbons due to their unique structure and properties. The large specific surface area of nano-carbons maximizes their active sites and accelerates electron transfer in catalytic reactions, helping them serve as direct surrogates to natural enzymes. This review presents insights into the recent advancements and key approaches towards the capability of nano-carbons as a catalyst to trigger advances in enzyme mimetics that have revolutionized the nanozyme sector. The structure–property relationship and unique features of nano-carbons regulating their catalytic behavior are also briefly discussed. Further, the respective mechanisms are summarized and discussed along with the applications of carbon-based nanozymes in different fields from biosensor design and environmental monitoring to therapeutics. The review concludes with the key scientific issues facing nano-carbons as catalysts and future perspectives on maximizing their benefits at the nanozyme nexus and beyond.

Received 12th January 2022,  
Accepted 3rd March 2022

DOI: 10.1039/d2ma00034b

rsc.li/materials-advances

### 1. Introduction

Enzymes are an essential part of human life and are bio-systems that facilitate a majority of biological reactions.<sup>1,2</sup> They do not reduce the activation energy for the acceleration of

<sup>a</sup> Department of Chemistry, Indian Institute of Petroleum and Energy, Visakhapatnam, Andhra Pradesh, 530003, India. E-mail: kumud@iipe.ac.in, kumud20010@gmail.com

<sup>b</sup> Mads Clausen Institute, NanoSYD, Smart Materials, University of Southern Denmark, Alision 2, Sønderborg 6400, Denmark



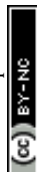
Nisha Dhiman

Nisha Dhiman earned her PhD in Chemistry from IIT Roorkee (2021), MSc (H.S.) degree in Chemistry from Panjab University, Chandigarh (2014), and BSc degree from HPU Shimla (S.V.G.D College Ghumarwin, 2012). She is currently working at the Sustainable Energy and Environmental Research Laboratory in IPE Visakhapatnam under Dr Kumud Malika Tripathi. Her research work is focused on the synthesis of green nanomaterials for application in energy storage devices, fuel cells, photocatalysis and enzyme mimetics.



Somnath Ghosh

Somnath Ghosh earned a BSc with honors in Chemistry (2005, University of Calcutta) and MSc in Chemistry (2007, Indian Institute of Technology (IIT), Delhi). From 2007 to 2012, he worked as a Research Scholar in the field of synthesis and characterization of biocompatible hybrid bio-nanomaterials in the Solid State and Structural Chemistry Unit (SSCU) of the Indian Institute of Science (IISc), Bangalore, and obtained a PhD in 2012. Currently, he is an Assistant Professor of Chemistry at the Indian Institute of Petroleum and Energy (IPE), Visakhapatnam, India. His research interests focus on biocompatible nanomaterials, biofilms, wound healing and carbon-based nanomaterials for energy application.



biochemical reactions, but rather provide an alternate path of lower activation energy to achieve high efficiency. Protein-based natural enzymes have high catalytic efficiency, biocompatibility, and high selectivity,<sup>3</sup> but they exhibit certain limitations when it comes to practical applications such as high cost, high susceptibility for contamination, limited working temperature, denaturation at high temperature, and poor recyclability.<sup>3–7</sup> With their confined nanostructures, unique optoelectronic/physicochemical properties, cost-effectiveness, high stability in harsh environments, ease of synthesis/purification, and rich surface chemistry, nanozymes have led to advancements in fields ranging from bio-sensing to biomedical applications as well as the chemical industry.<sup>8–10</sup> Nanozymes have integrated the beneficial properties of engineered nanomaterials and naturally occurring enzymes.<sup>11,12</sup> They work on the same principle as natural enzymes and are the best alternative to expensive natural enzymes due to their higher catalytic stability.<sup>13</sup> Moreover, the catalytic activity of nanozymes can be easily tuned by the precise engineering of their morphology, functional group, and composition.<sup>14</sup> The term “nanozymes” was first proposed by Scrimin, Pasquato, and co-workers.<sup>15</sup> Breakthrough work on nanozymes was done by Gao *et al.* when they investigated the peroxidase-like activity of ferromagnetic nanoparticles.<sup>16–18</sup> Nanozymes find applications in diverse fields such as sensing, biomedicine, environmental science, food safety, electrocatalysis, chemical production, fuel cells, and bioanalysis.<sup>8,19–24</sup>

Nanozymes include a class of functional nanomaterials that catalyze four basic biochemical processes. Diverse nanomaterials have been explored to mimic the catalytic properties of natural enzymes, which include metal nanoparticles,

metal–organic frameworks (MOFs), inorganic nanomaterials, covalent organic frameworks (COFs), metal and transition metal compound-based nanomaterials, supramolecules, biomolecules, and nano-carbons.<sup>8,21,25–27</sup> Zhang *et al.* have reviewed the research progress in the design, optimization, and application of diverse biomimetic nanozymes.<sup>25</sup> Among the various nanomaterial-based nanozymes, nano-carbons have gained huge research attention due to their rich chemical versatility, metal-free nature, low toxicity, high stability, and extraordinary electronic and optical properties. The most important advantage is that they can be easily synthesized at the gram scale by a simple and facile method.

The nano-carbons are composed of covalently bonded carbon atoms with different hybridization states ( $sp$ ,  $sp^2$ ,  $sp^3$ ), which deliver a huge diversity in morphology and structures. Mainly, they include fullerene, graphene, carbon-nitride, carbon-dots (CDs), carbon nanotubes (CNTs), carbon nanorods (CNRs), carbon nanowires, graphene nanoribbons (GNRs), and carbon quantum dots (CQDs). The exceptional properties and versatile physiochemical characteristics of nano-carbons provide opportunities for the immense development of enzyme mimetic applications.<sup>1</sup> These nanozymes have various applications in the field of bio-sensing, biocatalysis, biofuel cells, heavy metal detection, environment monitoring and remediation, medicine, antibacterial, antifungal treatment, and others.<sup>8,20,23</sup> Up to now, doping, surface functionalization, structural defects, size, and shape engineering of nano-carbons are the main strategies for tuning their  $\pi$ -system to achieve good performance as nanozymes.<sup>8</sup> The nano-carbons-based nanozymes can also act as photocatalysts, which can harvest solar energy for photocatalytic reactions.<sup>28</sup> For future



**Yogendra Kumar Mishra**

*technologies, including using them as novel templates to create hybrid and/or new 3D materials. Smart Materials Lab is developing tetrapod-based spongy materials for advanced technologies. He has published >230 papers, which have been cited >11 400 times with an H-index of 59.*

*Yogendra Kumar Mishra is a Professor MSO at the Mads Clausen Institute University of Southern Denmark, Sønderborg. Previously, he led a group at Kiel University, Germany, where he did Habilitation (2015) in Materials Science. He received a PhD (2008) in Physics from JNU, New Delhi, India. He introduced the flame process for tetrapod-nanostructuring and their 3D networks, which found many applications in different*



**Kumud Malika Tripathi**

*Lorient, France, and IIT Kanpur, India. Her research activities include the green synthesis of multifunctional nanomaterials for energy, healthcare and environmental applications. Kumud works at the interface of chemistry, material science and biology, exploring new nanomaterial-based strategies for environmental monitoring and remediation, self-recharge power units, energy storage devices, CO<sub>2</sub> capture and conversion, flexible electronics and photocatalytic water splitting for green hydrogen production.*

*Dr Kumud Malika Tripathi is a Ramalingaswami faculty/Assistant Professor in the Department of Chemistry, Indian Institute of Petroleum and Energy, Visakhapatnam, India. She earned her PhD in Chemistry from the Indian Institute of Technology, Kanpur, in 2013. Before joining IPE, she held several positions, including Assistant Professor in Gachon University, South Korea, postdoctoral fellow at the University of South Brittany,*



sustainability, natural bio-resources, waste material, and pollutant soot-derived nano-carbons constitute an important aspect in wide applications with economic advantages.<sup>29–31</sup> The exploration of sustainable nano-carbons have enriched the nanozyme field with potential applications of different components and structures in a cost-effective and environmentally friendly manner.

In the past two decades, there has been a plethora of studies on the fabrication of nano-bio interfaces, taking advantage of the unique optical, electrical, thermal and biocompatible properties of nano-carbons. However, technical and biological challenges exist regarding the biosafety and cytotoxicity of nano-carbons. Biomass-derived nano-carbons, especially CDs, CQDs, and GQDs, are a new promising option, since they have proven to have a negligible cytotoxic effect and higher biocompatibility than pristine nano-carbons.<sup>32,33</sup> Modification of pristine nano-carbons with biomolecules/biopolymers has also been proven to impart biocompatibility,<sup>32,33</sup> which clearly indicates that sustainable nano-carbons are safer for biomedical use, especially with enzyme mimetic applications. Another issue regarding the practical application of nano-carbons is the balance between production cost and performance. These biomass or waste materials-derived nano-carbons have acquired a global strategy in the current time for a wide variety of applications because of their cost-effective nature and environmental compatibility.<sup>34–38</sup>

In this review, we have focused on the nano-carbon-based nanozymes, mechanism of nanozymes for different catalytic reactions, factors affecting catalytic properties, and applications of nano-carbons for natural enzyme mimetic behavior. Furthermore, the versatility and capability of nano-carbons-based nanozymes in energy, environment, and healthcare applications have been described. Combined with the recent research status, the challenges and future opportunities at the leading edge are put forward.

## 2. Types and fundamentals of nano-carbon-based nanozymes

In the cellular-metabolism process, enzymes catalyze the production of reactive oxygen species (ROS), including superoxide radicals ( $O_2^{\bullet-}$ ), peroxide radicals ( $O_2^{\bullet 2-}$ ), hydroxyl radicals ( $OH^{\bullet}$ ), hydroperoxyl radicals ( $OOH^{\bullet}$ ), and  $H_2O_2$ .<sup>39,40</sup> These ROS take part in different cellular activities, like signal transduction, neurogenesis, cell proliferation/differentiation/migration and managing body defense against pathogen attack.<sup>41</sup> However, the excess production of these ROS can cause damage to cells and dysfunctions in normal cellular activities. These excess ROS can lead to dangerous diseases like cancer, skin issues, inflammation, and others. The enzymes generally involve the oxidation and reduction mechanism to catalyze the ROS. The nanozymes can mimic the natural behavior of enzymes for doing the same processes, and can modulate ROS generation and scavenging.

The existing nano-carbon nanozymes are divided into four categories, namely peroxidase, oxidase, catalase, and

superoxide dismutase (SOD). The catalytic activity of nano-carbon nanozymes is regulated by their morphology, surface structure, edge structure, surface functionalities, composition, and density of active sites.<sup>39</sup> The affinity of nanozymes to a particular substrate is closely related to the surface charge, functional groups, and active surface area. Nanozymes have a distinct reaction mechanism from their counterpart natural enzymes, which usually exhibit three successive steps: substrate adsorption, reaction, and product desorption.<sup>42</sup>

Nano-carbons are used as peroxidase mimics for the oxidation of many chromogenic substrates, including 3,3',5,5'-tetramethylbenzidine (TMB), 1,2-diaminobenzene (OPD), and 2,2-azino-bis(3-ethylbenzothiazoline-6-sulfonic acid) diammonium salt (ABTS), and nicotinamide adenine dinucleotide hydrogen (NADH) in the presence of  $H_2O_2$ . The decomposition of hydrogen peroxide results in the generation of water and oxygen, where it acts as an electron acceptor medium.<sup>1</sup> Mechanistically, nano-carbon nanozymes generate ROS, which further oxidizes a substrate. However, the composition and surface structure of the nanozymes significantly influence the mechanism of action. Oxidase enzyme produces water and  $H_2O_2$  by utilizing the electron acceptor and electron donor behavior of oxygen and hydrogen, respectively. As the name suggests, oxidases performs the oxidation of materials in the presence of  $O_2$ .<sup>1</sup> The visible light response of nitrogen-doped CDs (CDs) (TA-NCDs) was used to mimic oxidase activity to target tumor cells (Fig. 1a).<sup>43</sup> The authors reported that pyrolytic nitrogen acts as an effective surface binder and active site.<sup>43</sup> The SOD enzyme is the most important antioxidant that reduces the ROS produced in the cells, hence reducing oxidative stress such as cell death, inflammation, tissue injury, and even aging.<sup>1</sup> SOD-mimicking nanozymes convert superoxide into  $H_2O_2$ , and consequently to  $O_2$  and  $H_2O$ .<sup>39</sup> Intrinsic radicals play a significant role for SOD mimicking in nano-carbons. Wu *et al.* used surface-functionalized activated charcoal nanoparticles (NPs) to investigate the influence of intrinsic radicals on SOD activity (Fig. 1d). The change in the intrinsic radical intensity is directly related to catalytic turnover.<sup>44</sup> The production of ROS is the result of peroxidase (POD) activities. At first,  $H_2O_2$  is adsorbed on the nanozyme surface, then  $OH^{\bullet}$  is generated *via* electron transfer between  $H_2O_2$  and the nanozyme. The surface-adsorbed  $H_2O_2$  is stabilized before the generation of any intermediate *via* a partial electron exchange interaction.<sup>45</sup> Furthermore, intermediate products can react with biomolecules or biologically active molecules and other substrates (Fig. 1c).<sup>46</sup> The catalase nanozyme activity is similar to SOD-like activity, which converts  $H_2O_2$  to  $H_2O$  and  $O_2$  (Fig. 1b).<sup>47–50</sup>

The characteristic electron transfer properties and surface characteristics including “active sites” are responsible for the origin of the enzyme mimetic activities of nano-carbons.<sup>54</sup> The enzyme mimetic activity of nano-carbons can be explained on the basis of the capability of producing  $^{\bullet}OH$  from  $H_2O_2$ .<sup>54</sup> Pristine nano-carbons do not exhibit much activity towards enzyme mimetics due to their neutral electronic environment. However, heteroatom doping, surface functionalization and



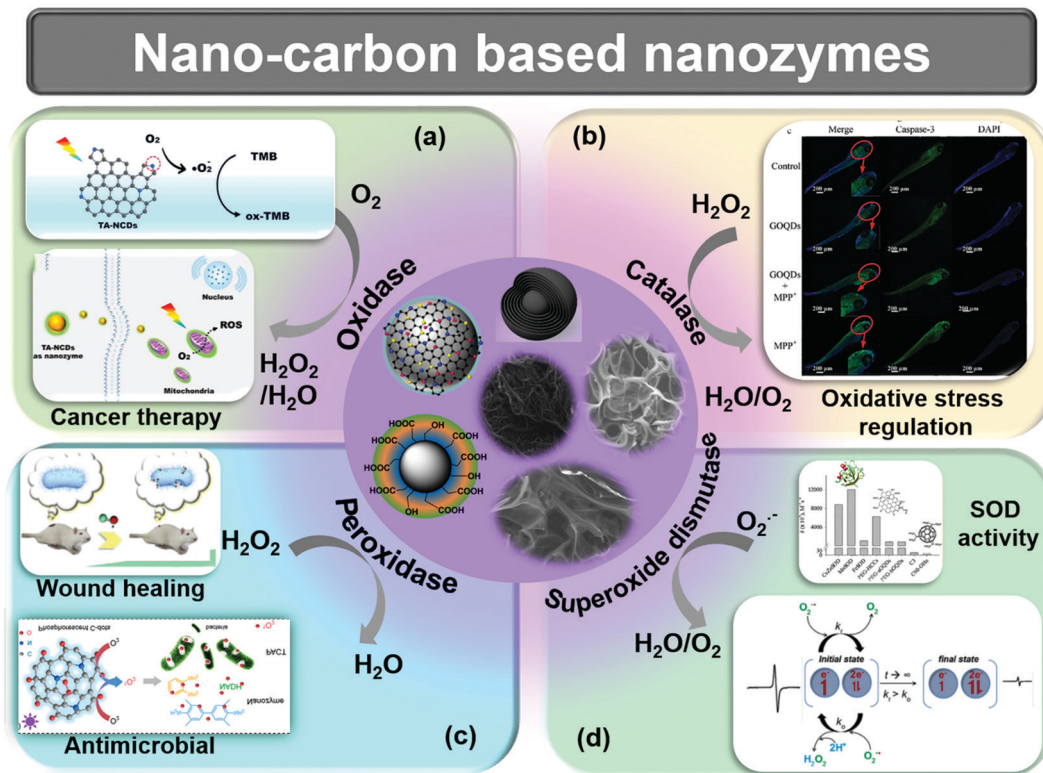


**Fig. 1** Schematic representation of the various types of nano-carbon based nanozymes, as well as basic catalytic reactions catalyzed by nanozymes. (a) Oxidase-mimicking activity and its application in tumor cell destruction.<sup>43</sup> (b) Catalase-mimicking activity and its applications in the regulation of oxidative stress.<sup>47</sup> (c) Peroxidase-mimicking activity and its application in wound healing<sup>51</sup> and antimicrobial activity.<sup>52</sup> (d) Comparison and mechanism of SOD-like activity.<sup>44,53</sup> Copyright American Chemical Society 2018, 2019, 2020; Copyright Elsevier 2020, 2021.

composite fabrication increase the charge carrier density and accelerate the electron transfer to substrate. In addition, surficial and structural modification can increase the asymmetry of spin density, which results in superficial electron transfer on the graphitic plane. It also decreases the energy gap of HOMO and LUMO, which is favorable for the ROS generation and hence to mimic enzymatic activity.<sup>55</sup> The uniform and porous structure, and hierarchical pores in the nano-carbons framework are also noticeable factors and driving forces for the acceleration of  $\cdot\text{OH}$  formation from the  $\text{H}_2\text{O}_2$  reduction.<sup>55,56</sup>

The above summarized nanozymes utilize the excessive ROS produced in the cell, *i.e.*,  $\text{O}_2^{\cdot-}$ ,  $\text{OH}^{\cdot}$ , oxygen, that result in the death of the cells.<sup>47</sup> Fig. 1 shows the reaction mechanism of basic nanozymes. The excess ROS in the cell or tissue leads to the death of the cell, which is the best for bacterial infection treatment, cancer therapy, retarding the microorganism growth, and maintaining hygiene. The utilization of nano-carbons as nanozymes is thoroughly and comprehensively listed here.

### 3. Factors affecting the catalytic activity of nano-carbon nanozymes

The performance of nano-carbons towards mimicking the activity of natural enzymes has been affected by various factors:

temperature, pH, elemental composition, heteroatom enrichment, textural properties (pore size, pore-volume, and pore size distribution), morphological changes, and edge defects.<sup>57–60</sup> The diversity of the carbon source, synthetic conditions, and routes lead to the structural/morphological assortment and multiplicity of nano-carbons.

#### 3.1. Effect of heteroatom incorporation

The doping of heteroatoms in nano-carbons is a widely used strategy for the tuning of their catalytic properties. The incorporation of heteroatoms in the nano-carbons by substituting carbon atoms changes the electrical neutrality of the framework, and hence enhances the nanozymes performance as shown in Fig. 2. The heteroatoms (N, F, P, S, O, and B, *etc.*) delocalize the total electron density of the framework by creating defects and acting as active sites for the substrate molecules.<sup>61–65</sup> The optical, electronic properties and chemical reactivity of nano-carbons can be tuned by the generation of n-type or p-type carriers. In addition, heteroatom doping can affect the water solubility and bandgap of nano-carbons. The carbon atoms located at the edge of the nano-carbons and adjacent to doped heteroatoms have been evidenced as intrinsic active sites for catalytic reactions.<sup>66</sup> Among the heteroatoms, boron is one of the electron-deficient elements with less electrons in the valence shell. The doping of B atoms in the porous carbon causes the carbon framework to become



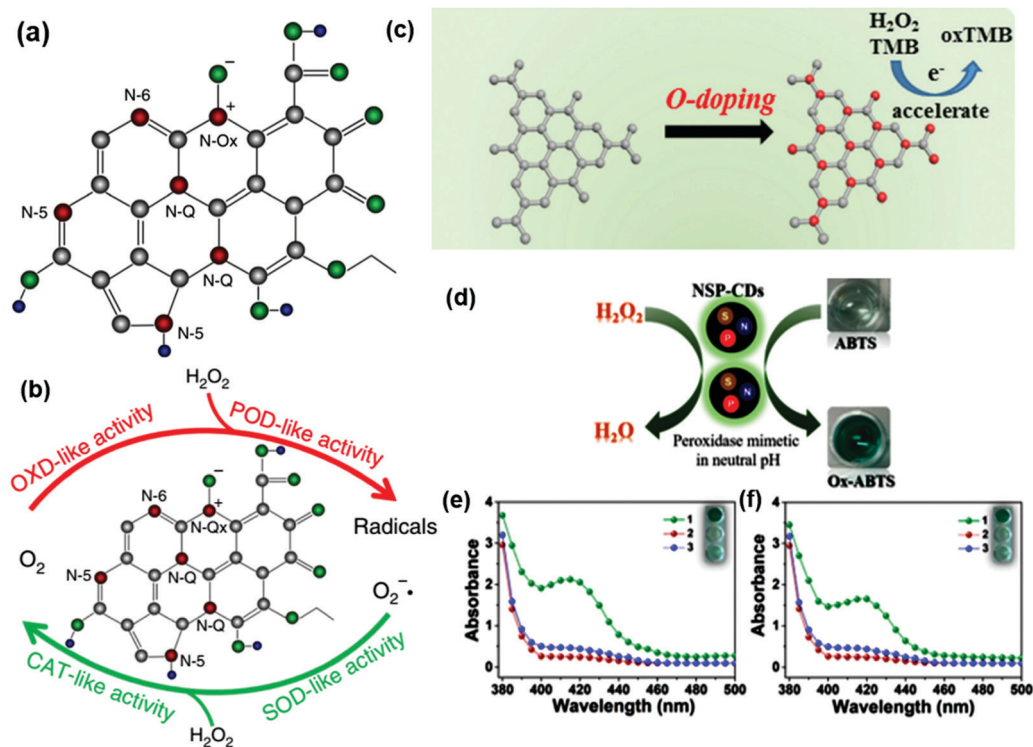


**Fig. 2** Heteroatom-doped nano-carbons for different nanozyme activities. (a) Schematic model of nitrogen and oxygen-containing surface functionality in N-PCNSs. (b) Schematic representation of the enzyme-like activities of N-PCNSs.<sup>70</sup> (c) Schematic diagram of the  $\text{H}_2\text{O}_2$  detection mechanism of OCN by accelerating electron transfer.<sup>71</sup> (d) Catalytic activity of NSP-CQDs. Schematic illustration of peroxidase-mimicking via ABTS oxidation. Peroxidase-like activity of NSP-CQDs under different parameters: (e) pH = 4 and (f) pH = 7. The absorbance spectra and digital images (insets) show the visual color changes of ABTS in different reaction systems: (1) ABTS +  $\text{H}_2\text{O}_2$  + NSP-CQDs, (2) ABTS +  $\text{H}_2\text{O}$  + NSP-CQDs, and (3) ABTS +  $\text{H}_2\text{O}_2$ .<sup>54</sup> Copyright American Chemical Society 2020; The Royal Society of Chemistry 2020.

electron-deficient, and makes active sites available for the substrates.<sup>67</sup> The nano-carbons-based nanozymes mainly consisted of hexagonal carbon rings, which attached to acetylene, vinylene, and others with  $\text{sp}^2$  and  $\text{sp}$  hybridization, respectively. Doping of heteroatoms could enhance the active sites to the substrates for decomposition and degradation, and the same has been proven by theoretical studies.<sup>68</sup> The electronegativity of B is 2.04, while that of C and N have 2.55 and 3.04, respectively, which make the B a more active center for the nanozyme activity. Jiao *et al.* have synthesized B-doped carbon-based Fe-N-C single-atom catalysts for the peroxidase mimic behavior, and showed its application for the detection of enzymes and other small molecules efficiently since B doping reduced the energy barrier.<sup>68</sup> Apart from B, the doping of P atoms in the framework could change the electronic environment of the carbon framework. Among the phosphorous compounds, phosphorene is one of the active members of the family. The doping of P atoms in the framework could change the polarization of the carbon framework and result in the occurrence of defects. These defects act as the active sites for the substrates for catalysis, and also enhance the conductivity of the nano-carbons.<sup>69</sup>

The N-doping leads to the formation of n-type nano-carbons due to their electron donor nature, which is highly active for the nanozyme activity as the lone pair of electrons participates in

the framework to perturb the electronic environment and produce defects and active sites. The doped nitrogen in the nano-carbons is of different types, *i.e.*, pyrrolic, pyridinic, graphitic, quaternary, and oxidized nitrogen (Fig. 2a).<sup>67,72,73</sup> Pyridinic N donates a p electron to the  $\pi$  system of the carbon framework, while pyrrolic N donates two p electrons to the delocalized  $\pi$  system, which consequently makes them highly catalytic active sites.<sup>51,74</sup> Graphitic N lacks a long electron pair since it coordinates to three carbons. The presence of a diverse electronic configuration to doped nitrogen significantly influences the absorbance energy of intermediates, and hence tunes the selectivity of the nanozymes.<sup>51,74</sup> In an innovative approach, Fan *et al.* showed that the N-doping in porous carbon nanospheres (N-PCNS) can be attributed to catalase, oxidase, peroxidase and superoxide dismutase activities, as shown in Fig. 2b. These N-PCNSs generate ROS, which were utilized to target the death of tumor cells.<sup>70</sup> Akin with B and P, the oxygen family is also highly active to enhance the activity of nanozymes. Zhu *et al.* synthesized ultrathin oxygen-doped carbon nitride (OCN) and tested it for peroxidase-like activity. The authors have suggested that oxygen doping has enhanced the activity by three times, which is attributed to accelerated electron transfer (Fig. 2c) compared to the pristine  $\text{g-C}_3\text{N}_4$ .<sup>71</sup> Another atom from the oxygen family is S, which contributes exceptionally towards the nanozyme activities. The doped S in the nano-carbons



framework helps in capping the electron, resulting in lower activation energy and leading to better catalytic performance.<sup>75</sup> The above discussed heteroatoms have their own unique properties, but out of all of these, nitrogen is best because of its half shell electronic configuration and presence of a lone pair.<sup>23,76–82</sup> The comparable atomic size of nitrogen and carbon makes it highly suitable for doping in the carbon framework.<sup>83</sup> These lone pairs act as electron donor sites, which make them an active site for substrate catalysis and provide a path with low activation energy.<sup>70,84</sup>

Although the doping of a single heteroatom in the nano-carbon framework makes it highly active for the nanozyme mimic behavior, the doping level and doping states are crucial parameters. The catalytic activity of nano-carbons as a nanozyme could be enhanced significantly by the binary or mixed doping of heteroatoms or metal or metal oxides. For instance, the co-doping of N, S and P was found to incorporate the peroxidase mimicking activity in CQDs (NSP-CQDs) by enhancing the active sites and ROS generation ability (Fig. 2d). In addition, heteroatom doping broadens the pH window due to the enhanced polarity and stability (Fig. 2e and f). These NSP-CQDs were also active at neutral pH towards ABTS oxidation and also exhibit antibacterial activity.<sup>54</sup> In another example by Luo *et al.*, co-doping with N and B enriched the edge structure. This resulted in enhanced structural defects and accelerated electron transfer between N to B, which acted as active sites for peroxidase activity.<sup>46</sup>

Liang *et al.* demonstrated the mechanism of peroxidase mimic activity by using both theoretical and experimental investigations. Based upon the P and N co-doping in the porous hollow carbon sphere nanozyme (PNCNzyme), they proposed a hypothesis to enhance the peroxidase mimicking activity.<sup>85</sup> The author used single and dual-doped graphene for the theoretical analysis. The P-doped graphene and N-doped graphene have comparable peroxidase activity for the rate-determining step. When the dual model is used, *i.e.*, P and N co-doped graphene, it shows 10.9 kcal mol<sup>-1</sup> of the rate-determining step, which is almost double for the single-doped graphene model. The synergy of P and N doping accelerates the peroxidase activity together instead of using a single heteroatom. In the same way, the theoretical investigation has been carried out for B, N, and S, N. The N atom has a lone pair of electrons, which enhances the reactivity towards the electron-donor and acceptor mechanism. However, the incorporation of the phosphorous atom has introduced defects that twist the atoms in the framework, as it has a large atomic radius resulting in big humps and pi-orbital axis vector (POAV) value in the sp<sup>2</sup> carbon atom, as shown in Fig. 3. The synergistic effects of the heterogeneous components in the nano-carbons facilitate electron transfer, enhance the substrate binding and active sites, and consequently enhances the selectivity and sensitivity of the nanozymes.<sup>85</sup>

### 3.2. Effect of size, morphology, and texture

The size and shape of the nano-carbon nanozymes is the key factor that affect and enhance the catalytic performance.<sup>31,86</sup> The specific activity of the nanozymes is significantly

dependent on the nano-carbon size and morphology. The adsorption of the analytes and reactant species is the first step in enzymatic reactions. Nano-carbons with smaller sizes exhibit a high surface-area-to-volume ratio and strongly adsorb reactant species. Furthermore, surface defects like dangling bonds, missing graphitic planes, steps, kinks, and edge effects are responsible for the generation of surface-active sites.<sup>46,87,88</sup> A decrease in the particle size also lowers the absorption energy, and hence increases catalytic efficiency. The edge-rich nano-carbons provide a diverse set of flexible tuning options for the engineering and design of nanozymes.<sup>66</sup> Compared to other 2D and 3D nano-carbons, the 0D nano-carbons provide a high surface-to-volume ratio, versatile surface functionalization, high density of active surface sites, and higher tunability in physiochemical properties. The nano-carbons of varying morphology, like nano-leaves, nanosheets, quantum dots, nano-flowers, nanoflakes, dendrites, core-shell structures, sponge, bamboo-like, nanotubes and nanosphere, were explored for the enzyme mimetic activity, as shown in Fig. 4.<sup>89,90</sup> The more exposed surface area of the tentacles of dendrites accelerates the catalysis by providing more surface-active sites. The core-shell morphology can impart the extra activity of the metallic core supported by CNTs<sup>91</sup> since the tubular morphology can provide both internal and external sites for enzymatic activity.<sup>77</sup> Furthermore, the pores of the spongy nanospheres have enhanced the activity, as pores are the active site for catalysis. The bamboo-like stacking of particles (such as CNTs) provides not only a porous upper surface, but also a long hollow space inside the tube, which acts as active sites for the substrates.<sup>89,90</sup>

Only a few studies are available, which focused on the influence of morphological variations on the enzymatic activity of nano-carbons.<sup>93</sup> Jiang *et al.* synthesized the B-doped carbon-based core-shell structure, where the iron NPs are the core and B-doped carbon acts as a shell. The authors investigated the B atom replacing the carbon atom at the edges. This resulted in the increment of the defects, hence acting as the active site in the core-shell structure and enhancing the peroxidase-like activity.<sup>94</sup> Recently, Sheng *et al.* synthesized water and oxygen-stable phosphorene-based microporous carbon. They suggested that the doping of phosphoric acid could generate microporous and large mesopores in the carbon framework. The good micro- and mesoporous structure of carbon makes the diffusion and transport of ions easy, and was further utilized as a nanozyme for the sensing of 8-hydroxy-20-deoxyguanosine.<sup>95</sup> The nanospheres-based carbon nanozymes synthesized by Fan *et al.* by doping N showed good catalytic activity for tumor therapy. These nanospheres provided a large surface area for the nanozyme to catalyze the substrate.<sup>70</sup> Bamboo-like morphology-based carbon nanozymes have been synthesized by He *et al.* for oxidase-like activity. Their investigation suggested the presence of hollow CNTs like bamboo with 10 nm in thickness, and the distance between the bamboo-like joints was 100 nm. These hollow CNTs were cobalt capped, which prevented the leakage of NPs and these tubes acted as nanoreactors for oxidase mimic activity.<sup>90</sup> The morphological changes also enhanced the catalytic activity. This concept was



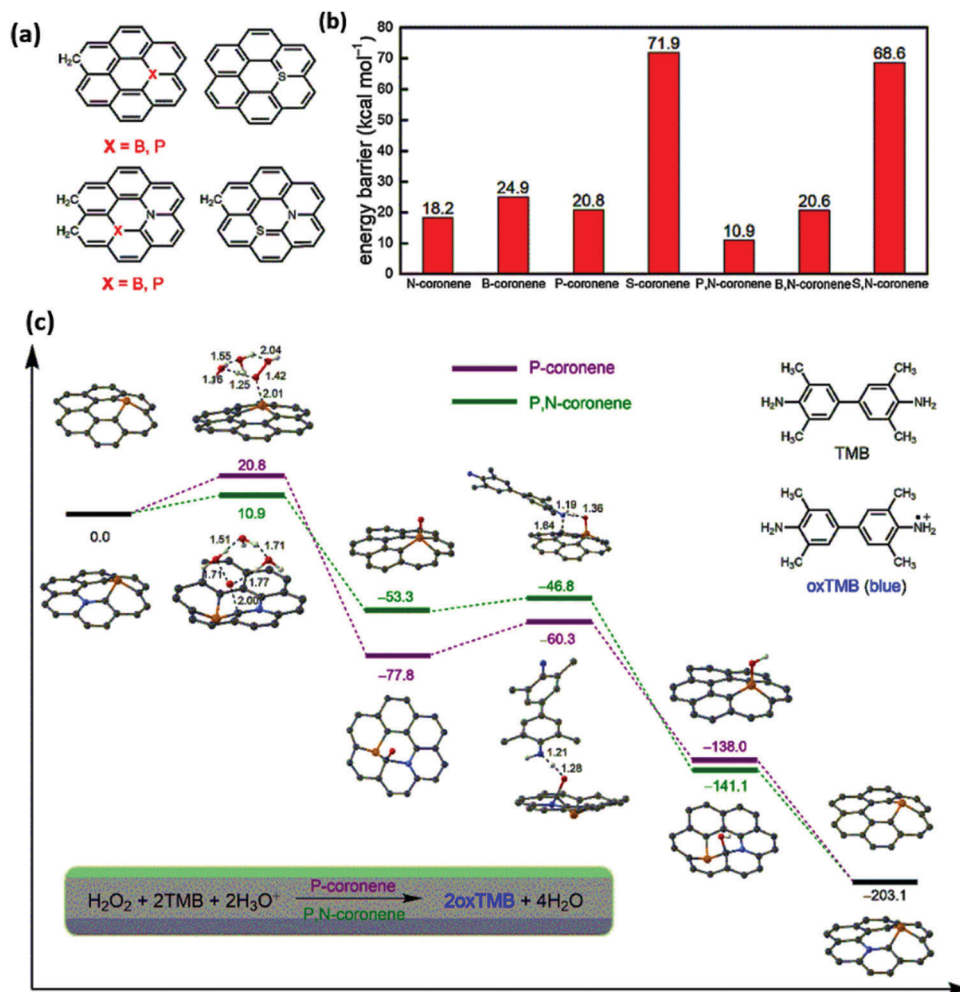


Fig. 3 DFT theoretical analysis of the peroxidase-like activity of metal-free carbon materials. (a) The geometric models for N, B, P, S single-doped and dual-doped graphene. (b) The energy barriers for the rate-determining steps of the peroxidase-like activity of N, B, P, S single-doped and dual-doped graphene. (c) Calculated reaction energy profiles corresponding to the peroxidase activity.<sup>85</sup> Copyright Elsevier Ltd 2020.

proved by Lin *et al.* by doping cerium in the carbon-based GO nanozyme. The doping results in defects and hence topology changes, which leads to the good catalytic performance of the nanozyme.<sup>92</sup>

### 3.3. Effect of surface functionalization

Catalytic reactions take place on the nano-carbons surface. At first, the substrate/analyte is adsorbed on the catalyst surface and then diffuses to the internal area. This is followed by the chemical reaction and final desorption from the catalyst, and the surface active sites are then regenerated.<sup>96</sup> The surface functional groups, surface electronic structure, and surface chemistry significantly affect the catalytic activity of nano-carbons. Surface modification varies from the dangling bond, functionalization, composite fabrication, small molecules, ions to macromolecules, and is recognized as a promising strategy to tune and regulate the nanozyme properties (Fig. 5a).<sup>96</sup> For instance, surface modification can enhance the tumor treatment efficiency of nanozymes.<sup>97</sup> Various strategies have been utilized for the modulation of selectivity and catalytic activity of

nano-carbons nanozymes by affecting their surface chemistry. The precise control of the surface functional groups can achieve selectivity for a particular substrate. In addition, the surface modification could broaden the suitable pH window and increase the pH stability.<sup>98</sup>

Pristine nano-carbons, such as fullerene, CNOs, CNTs, and nano-diamonds, are highly insoluble in water, which can absorb free radicals based on their delocalized  $\pi$  framework. However, their lack of solubility restricts their direct utilization in enzyme mimicking. The surface functionalization with oxygenated functional groups or other hydrophilic moieties, such as monomeric or polymeric amines, is a widely used strategy to impart the water solubility and tune the physiochemical properties of nano-carbons.<sup>99–101</sup> Sun *et al.* conducted a series of studies to investigate the influence of carbonyl, carboxylic, or hydroxyl groups on the peroxidase-like catalytic activity of graphene quantum dots (GQDs).<sup>102</sup> The deactivation of  $-\text{COOH}$  did not show any decrease in catalytic activity, while the deactivation of  $-\text{OH}$  and ketonic carbonyl groups increased and decreased the catalytic activity of GQDs, respectively.



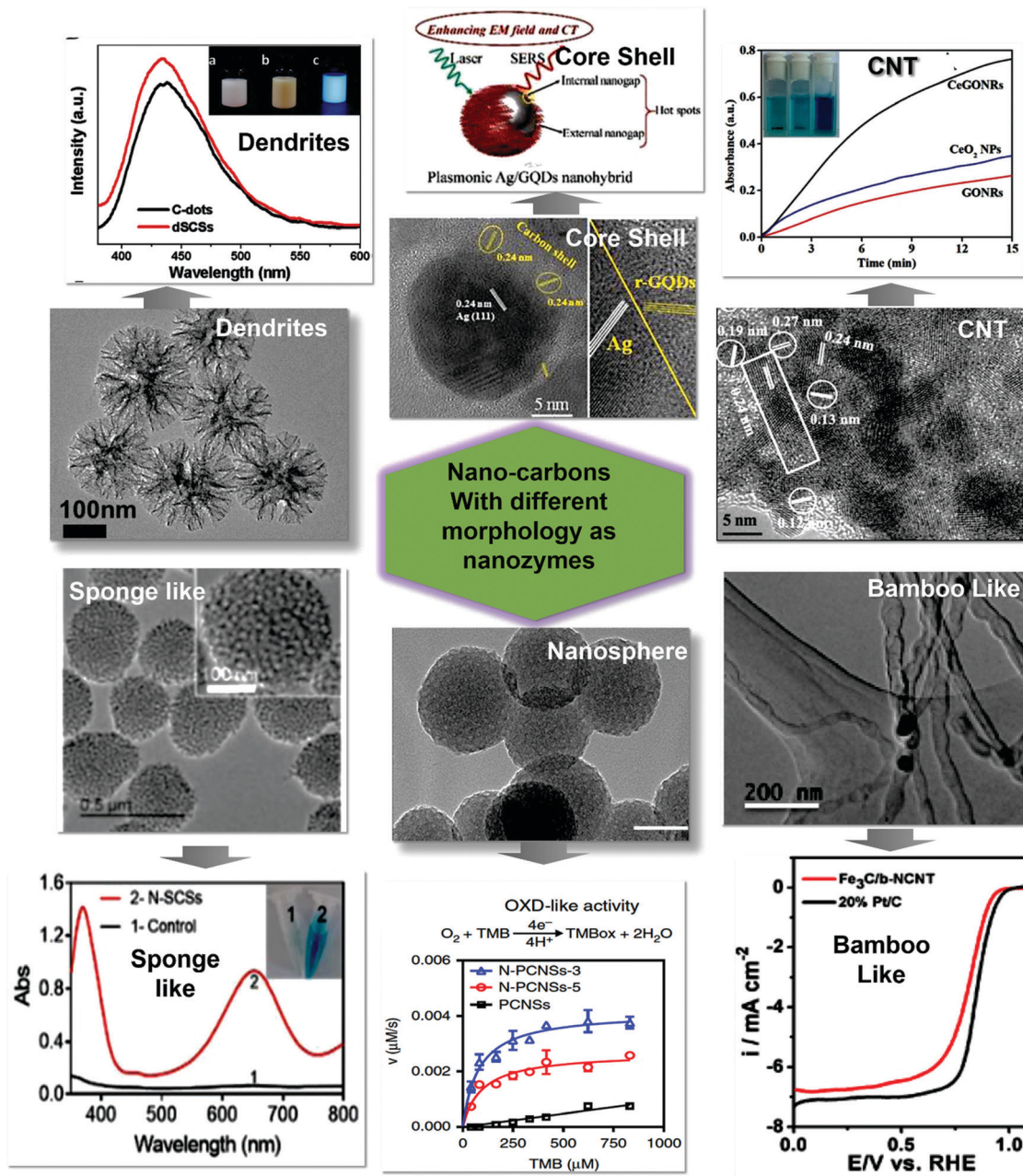


Fig. 4 Different morphologies of nano-carbon nanozymes and the effect of morphology on the nanoenzymatic activity.<sup>7,70,82,89,91,92</sup> Copyright Elsevier Ltd. 2021; The Royal Society of Chemistry 2019, 2020.

This indicates the considerable influence of the carbonyl groups (C=O) on the enzymatic activity of nano-carbons. The -COH groups can act as catalytic inhibitor sites and -COOH enhances the interaction with the substrate.<sup>102</sup>

The -COOH group exhibits a significant influence on SOD-like activity due to its strong affinity to ROS *via* hydrogen bonding. When the second ROS are in proximity of such nano-carbon-COOH-ROS adducts, it is disproportionated to O<sub>2</sub>, •OH, or H<sub>2</sub>O<sub>2</sub> either by taking the protons from carboxyl groups or water molecules.<sup>98</sup> The peroxidase-like catalytic activity of GQDs was found to be much higher than GO toward

the oxidation of TMB. The increase in activity was achieved by the increase in the density of functional groups and hence high catalytic sites, and superior electron transportation activity.<sup>103</sup> Another study by Song *et al.* showed that carboxyl-modified GO exhibited higher peroxidase-like activity than HRP.<sup>104</sup> ROS regulation efficiency and neuroprotective effects of GO were increased in 1-methyl-4-phenyl-pyridinium ion (MPP<sup>+</sup>)-induced PC12 cells mimicking catalase-like activity when it converted into GOGQDs. GOGQDs decrease the ROS levels by 43.6% and 90.6%, and caspase-3 activities decreased by 30.4% and 32.6% in the heart and head of zebrafish, respectively, as shown in





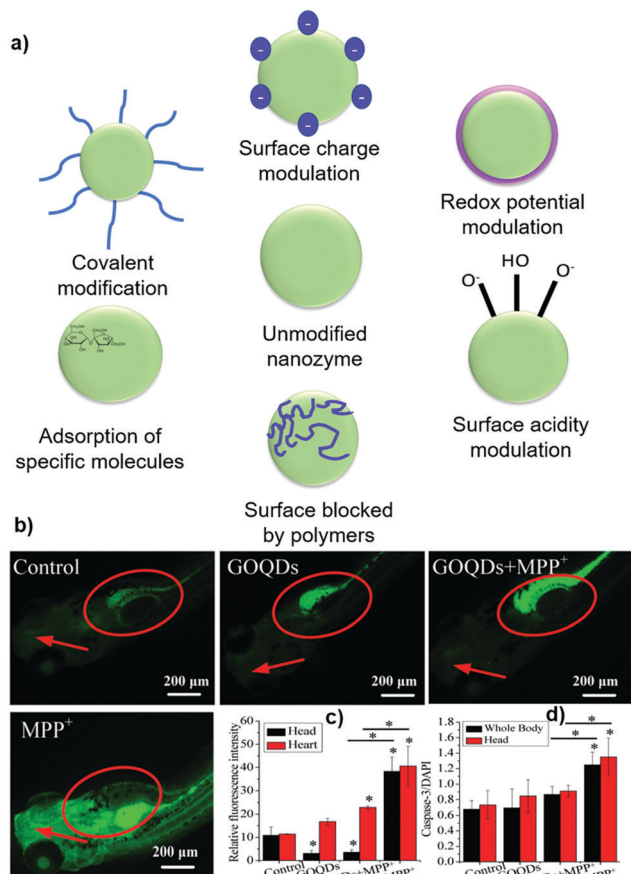


**Fig. 5** (a) Schematic showing a few general strategies and effects of modulating the enzyme-like activities of nanomaterials *via* surface modification.<sup>96</sup> Effects of GOQDs on MPP<sup>+</sup>-induced oxidative stress and apoptosis *in vivo*. (b) Heads and hearts of larvae. The heads and hearts are indicated by red arrows and circles, respectively. (c) Quantitative analysis of the relative fluorescence intensity of ROS in the heads and hearts of the larvae. (d) Quantification of caspase-3 levels in the whole body and head of larvae.<sup>47</sup>

**Fig. 5b–d.**<sup>47</sup> Incorporation of bimetallic shells over hollow-core particles impart some new properties with the combination of intrinsic properties. Core-shell modifications are beneficial towards the enhancement of plasmonic effects, optical properties, charge separation, and biocompatibility.<sup>105</sup> The peroxidase-like activity of the core-shell nanostructure of Ag/Au over the GO core was also used for the electrochemical detection of H<sub>2</sub>O<sub>2</sub>. The incorporation of Ag and Au significantly enhances the sensitivity of GO.<sup>105</sup>

## 4. Designs and advancement in nano-carbon based nanozymes

Nano-carbons-based nanozymes are emerging, as they are metal-free, which reduces the toxicity, in addition to having high stability, sustainability, good textural and morphological properties, biocompatibility, environmentally benign properties, and high active sites for the catalysis.<sup>98</sup> The method of synthesis of the nano-carbons nanozyme has been summarized in Fig. 6,

which affects the performance of the nanozymes.<sup>26,38,106–110</sup> The high temperature and pressure conditions could affect the morphology and physicochemical properties, and provide high surface area, more active sites, high chemical, and thermal stability, which generally limits the enzymatic activities in natural enzymes. The different solvents used in the synthesis also change the textural properties and enhance the surface roughness for the high active sites. The electrochemical route provides impurity-free nano-carbon nanozymes with controlled morphologies of nanostructures.<sup>111</sup> The combination of two or more techniques, such as solvothermal, self-assembly, ultrasonication and thermal activation, can result in a confined structure with a high density of active sites.<sup>112</sup> The variation in the carbonization time and temperature during hydrothermal carbonization can affect the morphology and yield of the nano-carbons (Fig. 6a).<sup>108</sup> A bio-inspired metal matrix composite having a brick and mortar structure was synthesized by Xiong *et al.* by using the impregnation method, as shown in Fig. 6b. This composite exhibited significantly higher strengthening efficiency and increased modulus.<sup>107</sup> An interesting approach by Lim *et al.* showed the nanoengineering of CNTs by twisting graphene sheets, and hence precise control over the chirality and reactivity (Fig. 6c).<sup>110</sup> The hydrothermal method was explored to control the porosity of the hollow carbon nanosphere for the enhancement of the catalytic sites (Fig. 6d).<sup>109</sup> The microwave plasma irradiation method is an efficient and environmentally friendly technique for the unidirectional growth and nucleation of nano-carbons. For instance, the CDs enriched with heteroatom have been synthesized by microwave method as shown in Fig. 6e.<sup>54</sup> The nano-carbon-based nanozymes that have different dimensional structures synthesized using different methods to mimic the enzymatic reactions are summarized in Fig. 7.

### 4.1 0-D nano-carbons-based nanozymes

The 0-D nano-carbons mainly include the CQDs or GQDs, and they have dimensions of ~10 nm or less.<sup>91</sup> Sun *et al.* coined the term CDs, and it was discovered by Xu *et al.*<sup>113</sup> CQDs are composed of a nanocrystalline core and oxygenated functional groups on an amorphous core, while GQDs are composed of a few layers of graphene or GO. The accidental discovery of the CDs has gathered the interest of researchers, which was isolated during the separation process of single-walled CNTs.<sup>114</sup> CDs are the class of NPs that are composed of sp<sup>2</sup> and sp<sup>3</sup> hybridized carbon atoms, *i.e.*, graphitic carbon and graphene/graphene oxide, respectively.<sup>115</sup> CDs can be synthesized using top-down and bottom-up approaches. In the top-down approach, carbon-based materials like graphene and fullerene were broken down by exploring different synthetic routes.<sup>12</sup> Meanwhile, in the bottom-up approach, the combustion and different annealing methods were used to carbonize the carbohydrates, polymers, and biomass to form CDs. Lv *et al.* synthesized the CDs-based nanozymes and further investigated their physicochemical properties to mimic the peroxidase-like activity of natural enzymes. The authors fabricated four different types of CDs from different metal-free precursors, *i.e.*, glucose,  $\alpha$ -cyclodextrin (CD),  $\beta$ -CD, and  $\gamma$ -CD.<sup>116</sup> A theoretical



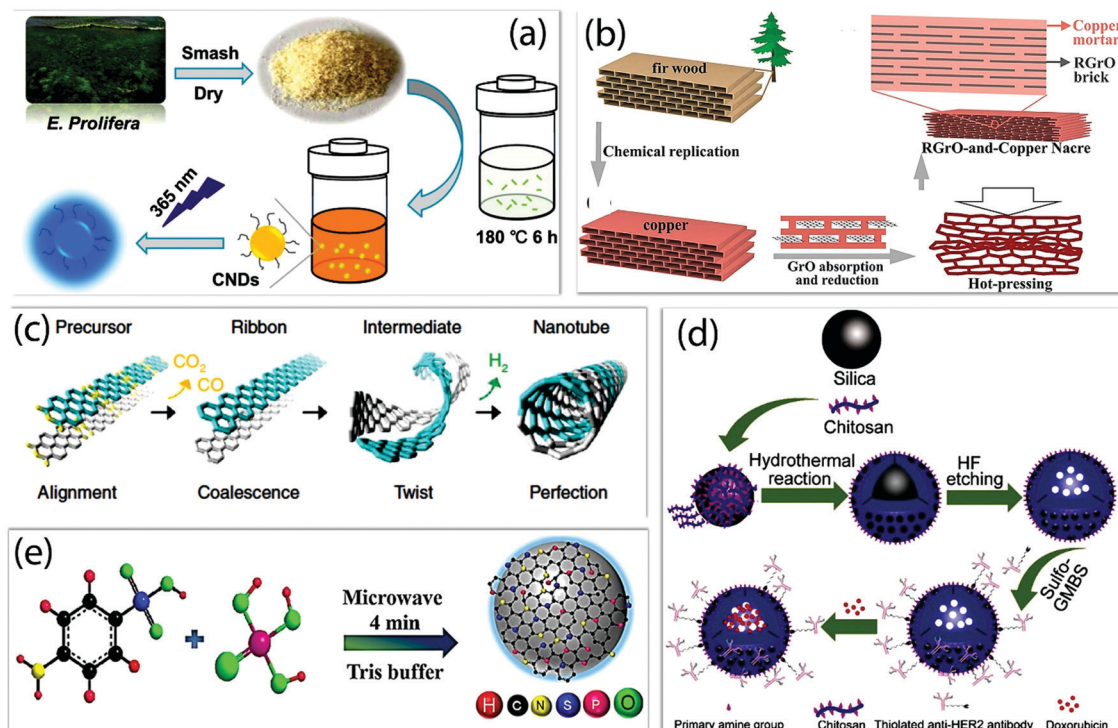


Fig. 6 Different methods for the synthesis of nano-carbon nanozymes. (a) Schematic illustration of CND generation via the hydrothermal treatment of *E. proliferata*.<sup>108</sup> (b) Schematic illustration of the synthesis of rGO-copper artificial nacre.<sup>107</sup> (c) Basic steps involved in the synthesis of CNTs via the twisted graphene nanoribbons path.<sup>110</sup> (d) Schematic depicting the synthetic process of HER2@HCNs/DOX. (e) Schematic illustration of N, S, and P codoped-CQD synthesis.<sup>54,107–110</sup> Copyright The American Chemical Society 2020, 2015; Royal Society of Chemistry 2017; Springer Nature 2017.

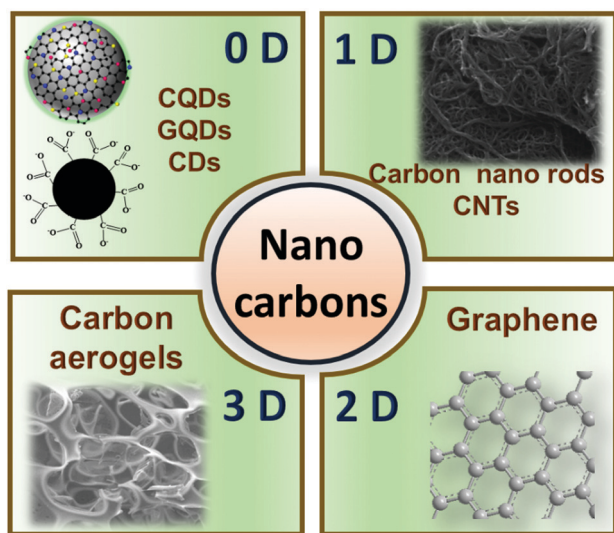


Fig. 7 Various architectures of nano-carbons.

investigation on the reaction kinetics suggest that all of the CDs have different catalytic performances with a substrate based on the surface charge, size, shape, and electrostatic interaction.<sup>12</sup> Although these nanozymes are metal-free, the doping or incorporation of functional groups other than metal or metal oxide could further enhance the activity. The doping of heteroatoms

(like N, P, S, O, B, and F) has enhanced the nanozyme properties. Zhang *et al.* synthesized the water-soluble nitrogen-doped CDs, and studied the photo-oxidation activity of these CDs by converting the triplet's oxygen into a singlet oxygen. This singlet oxygen acts as a photosensitizer, which further mimics the oxidase-like activity by oxidizing TMB, NADH, and OPD.<sup>52</sup> Recently, Acharya and co-workers synthesized a nitrogen-doped metal-free functionalized nanozyme LC-CNS@NTA. The solubility of LC-CNS had been enhanced by treating it with ethylenediamine (EDA) and nitrilotriacetic acid (NTA). It was observed that the exposed  $-\text{COOH}$  groups in the NTA had enhanced the solubility compared to the EDA groups, which consisted of  $-\text{NH}_2$  as their terminal groups. The NTA exposed surface groups developed a nanosphere that provided a high surface area for the catalysis. They further utilized this nanozyme for the peroxidase activity on the OPD, TMB, and  $\text{H}_2\text{O}_2$  substrates. It also acts as a catalase mimic enzyme.<sup>117</sup>

Furthermore, the doping of the metal or metal oxide along with heteroatoms could enhance the catalytic activity of the nano-carbon nanozymes. The CDs can act as nanozymes for light-controlled oxidoreductase-like activity. Zhao *et al.* designed CDs-based nanozymes, which were doped with nitrogen and gold (Au/NC), and further investigated their redox behavior towards light-controlled processes. These N-Au doped CDs showed a synergic mechanism of photoexcitation and surface plasmon resonance, respectively. In particular, the doping of gold was found to reduce the fluorescence emissions



by acting as a quencher. The SOD-like activity of these nanozymes significantly reduces the ROS concentration and makes it an efficient antioxidant. The mechanism was studied by the generation of  $\cdot\text{OH}$  with the help of a Fenton reagent. The radicals are responsible for the strong fluorescence emissions centered at 435 nm in the absence of Au/NC, while the emission was reduced in the presence of a catalyst.<sup>118</sup> Furthermore, the synthesis methods can significantly influence the activity of the nano-carbon nanozymes. Herein, Dong *et al.* synthesized the enzyme-like CDs (e-CDs) *via* the solvothermal method in *N,N*-dimethylformamide (DMF). The synthesized e-CDs were utilized for the inhibition of oxidation and acted as a radical scavenger. These e-CDs reduced the oxidative stress and suppressed the anti-aging phenomena by investigating the conversion of  $\text{Fe}^{3+}$  ions to  $\text{Fe}^{2+}$ , and experimented with both *in vivo* and *in vitro* methods for demonstration.<sup>119</sup>

#### 4.2. 1-D nano-carbon-based nanozymes

The one-dimensional (1D) nano-carbons generally include CNTs and CNRs. The 1-D materials are the ones that have one dimension out of the nanoscale. In 1991, Sir Iijima discovered CNTs and suggested that when the carbon is in an  $\text{sp}^2$  hybridization state, it can form a different graphitic structure.<sup>120</sup> The CNTs include single-walled carbon nanotubes (SWCNTs) and multi-walled carbon nanotubes (MWCNTs).<sup>121</sup> The CNTs and other 1-D nano-carbons-based structures have shown high activities in mimicking the natural enzymes. Earlier, Qu and co-workers synthesized the metal-free SWCNTs that can catalyze the oxidase-like activity and mimic horseradish peroxidase (HRP). These nanotubes show pH, temperature, and  $\text{H}_2\text{O}_2$  concentration-dependent HRP-like activity.<sup>122</sup> Zhang *et al.* synthesized the 1-D core-shell structure to mimic the activity of the natural enzyme. The solvothermal method was utilized for the synthesis of the  $\text{Fe}_3\text{O}_4@\text{C}$  core-shell nanostructures. This nanozyme was further explored for the colorimetric detection of PDGF-BB with a detection limit of 50 aM, and was also explored for the peroxidase-like activity.<sup>123</sup> Another study on the 1-D core-shell structure has been documented by Peng *et al.*, who synthesized the  $\text{Fe}_3\text{O}_4@\text{C}/\text{Ni}$  nanocomposites. The synthesized nanocomposite showed the nanotube-like morphology, and the hollow porous structure contributes toward the superior enzymatic activity. This hybrid nanostructure can detect cholesterol in the blood from 5 to 200  $\mu\text{M}$ , and can go up to the lower detection limit of 0.17  $\mu\text{M}$ . In this procedure, the synthesized nanozyme in the presence of  $\text{H}_2\text{O}_2$  showed a visible color change during the conversion of cholesterol molecules to cholest-en-3-one by oxidation.<sup>124</sup> The enzymatic activity of  $\text{Fe}_3\text{O}_4$  NPs is good, but the toxic nature puts them aside, which makes  $\text{Fe}_2\text{O}_3$  the best alternative for doping in nano-carbon. Yang *et al.* synthesized  $\text{Fe}_2\text{O}_3$ -doped CNTs and utilized them for the sensing of dopamine, which is an important neurotransmitter. The authors utilized the atomic layer deposition method for the deposition of  $\text{Fe}_2\text{O}_3$  on CNTs, and confirmed it by high-resolution transmission electron microscopic analysis (HR-TEM). The peroxidase activity was significantly enhanced in comparison to pristine CNT and

$\text{Fe}_2\text{O}_3/\text{CNT}$ .<sup>125</sup> Furthermore, Gally *et al.* functionalized CNTs with avidin, which is a protein that binds biotin, and formed a nanocomposite with ruthenium NPS. The synergic effect of the synthesized composites reduced  $\text{H}_2\text{O}_2$  efficiently.<sup>111</sup> The functionalized CNTs with Prussian blue were synthesized by He *et al.* and utilized as a cholesterol oxidase nanozyme for the detection of cholesterol. The Prussian blue was dispersed onto the precleaned MWCNTs with high hydrophilic groups. Here, the nanotubes acted as a support for Prussian blue and also as a reducing agent for  $\text{Fe}^{3+}$ .<sup>126</sup>

#### 4.3. 2-Dimensional nano-carbon nanozymes

The class of 2-D nano-carbon-based nanozymes mainly includes graphdiyne, carbon nanosheets, and graphene.<sup>127</sup> Geim and co-workers were the first to separate graphene from the 3-D graphite, and this led to the extraordinary research area. Graphene has a honeycomb-like 2-D structure with  $\text{sp}^2$  hybridized carbons and high thermal stability.<sup>128</sup> The discovery of graphene in 2004 led to the attention of researchers, and this 2-D structure has since been utilized in many fields like the energy sector, adsorption, catalysis, detection, and others.<sup>31,129–131</sup> The nano enzymatic activity of graphene has been studied extensively. In this direction, Zhu *et al.* synthesized heteroatom-doped graphene as a sensor for the detection of pesticides. The authors masked the nanozymes with the different pesticides and utilized the peroxidase mimic activity of graphene as a sensor. The masking of pesticides decreases the activity of the nanozyme, which helps in the colorimetric detection of different pesticides.<sup>83</sup> Another important class of graphene is graphene derivatives and their composites with metal or metal oxide, which could further enhance the enzymatic activity of nanozymes. Pandit *et al.* synthesized the graphene derivative by utilizing the one-pot synthesis method, where they explored the bottom-up approach. 2,4,6-Tribromo-3-hydroxybenzoic acid has been utilized for the synthesis of water-soluble 2D nanosheets. These nanosheets show the peroxidase mimic behavior, and they could be used as an assay for NADH and dopamine.<sup>132</sup> Another report on 2D carbon nanosheets has been documented by Hou *et al.*, who doped 2D carbon nanosheets with Cu and N, which is highly active for the peroxidase activity. The encapsulation of Cu and N in the carbon nanosheets has been confirmed by SEM, and the homogenous doping of both the elements has been recorded. The Cu-N-doped carbon nanosheets synthesized at 700 °C showed the highest activity due to the high degree of defects. Meanwhile, above this temperature, the activity was decreased because of the removal of N from the framework.<sup>133</sup> Zhu *et al.* utilized the voltammetric technique to analyze the enzymatic activity of the carbon nano-horns phosphorene nanocomposite. The carbon nano-horn provides high electrical conductivity with good electron transport and low impedance.<sup>134</sup> Li *et al.* utilized the 2-D carbon nanosheets for embedding the mixture of cobalt and zinc NPs to mimic the oxidase activity. The synthesized nanosheets have a leaf-like structure and defective graphene framework, which enhances the catalytic activity and



accelerates electron transfer between the catalyst and substrate for TMB oxidation.<sup>127</sup>

Graphene oxide (GO) was also investigated for nano enzymatic activity by many research groups.<sup>135,136</sup> Another important class of 2-D material is graphitic carbon nitrides, graphdiyne (GYD), which were reported by different research groups to mimic the different enzymatic activities.<sup>137–141</sup> Among other allotropes of carbon, GYD is one of the newest and most emerging synthesized forms. Graphdiyne consists of the alternative units of a benzene ring and acetylene unit with  $sp^2$  and  $sp$  hybridized carbon, respectively. The porous structure and controlled morphological properties lead to the formation of active sites for catalysis.<sup>142</sup> Bi *et al.* synthesized the heteroatom-doped GYD with hydrothermal method by using sodium borohydride as a source of B. The doping of B is attributed to a large number of defects in the graphene framework, which could be the active site for peroxidase activity. They studied the doping site of B in GYD, and the Gibbs free energy diagram revealed the high reactivity of the catalyst when B was doped on the outer side of the ring.<sup>67</sup> Deep insights on the GDY-based nanozymes have been provided by Wang *et al.*, where they synthesized the palladium and iron-based nanosheet and utilized GDY as a support for NPs for *in vivo* and *in vitro* anti-bacterial activity with oxygen-scavenging properties.<sup>120</sup>

#### 4.4. 3-D nano-carbon nanozymes

The 3-D nano-carbons nanozymes mainly include the hybrids of graphite, graphene aerogels, carbon aerogels, graphene foam, and others.<sup>143</sup> These nanostructures could form composites/hybrids with MOF, COF, metal oxides,  $MoS_2$ , and others. Recently, Chen and co-workers synthesized the 3D composite of  $MoS_2$  and GO.  $MoS_2$  acts as a highly active species for enzymatic activities, which are arranged vertically between the rGO layers acting as a substrate for  $MoS_2$  growth. Both theoretical and experimental studies have suggested that the defects created by molybdenum and sulfur in  $MoS_2$  have enhanced the sensitivity and detection efficiency.<sup>144</sup> The one-pot synthesis method has been explored by Wang *et al.* for the synthesis of 3D graphene nanocomposites of  $Fe_3O_4$ . The 3D structure leads to the generation of channels and voids, which could act as catalytic active sites.<sup>145</sup> Furthermore, to enhance the activity of graphene, the mesoporous  $Fe_3O_4$  has been incorporated and a 3D structure has been designed by Qiu *et al.* for the detection of *p*-nitrophenol as it is an industrial effluent.<sup>146</sup> To enhance the enzymatic activity of 3D nano-carbons, the doping of small molecules has been done. In this line, Cai *et al.* have incorporated phytic acid in the graphene to make it porous and active for the superoxide mimic activity. The sensitivity of the synthesized composite was checked against different materials present in the living cell, but the nanozyme exhibited maximum current response for the superoxide anion. This high current response was exploited for the detection of the superoxide anion in the living cell.<sup>147</sup> The Zeolitic imidazolate frameworks (ZIFs)-based nano-carbons were also utilized as nanozymes. Mou *et al.* designed the multilayer ZIF-based N-doped carbon

(BSA-PtAu@CNS) for the tandem catalysis. The BSA-PtAu@CNS nanozyme oxidizes glucose into gluconic acid, producing  $H_2O_2$ , and the TMB substrate oxidizes, which shows the colorimetric detection of glucose.<sup>148</sup> The 3D graphene and CNTs-based carbon nanozymes have been reported by many groups and utilized further for detection, sensing, environmental application, and others.<sup>89,149,150</sup> The electrochemical sensing and detection of dopamine was carried out by Lu *et al.* under real sample conditions without the use of hydrogen peroxide for oxidase activity. They fabricated a Co, N co-doped hierarchical hybrid (Co@NCNTs/NC) composite from ZIF, which showed intrinsic oxidase activity without the use of  $H_2O_2$ .<sup>151</sup> Pt nanoclusters (Pt NCs) grafting on the 3D graphene foam attributed high oxidase-like activity towards the oxidation of TMB, and also polyphenol oxidase (PPO) mimicking activity. The synergy between Pt NC and graphene foam provides the higher catalytic sites for the diffusion of substrates and accelerated electron transfer for redox reactions. This nanozyme shows excellent selectivity and high sensitivity for the catechol oxidation confirmed by mixing different phenols and ions into the solution.<sup>152</sup>

A simple self-assembly-based fabrication of the 3D hydrogel using GO, poly(vinyl alcohol) (PVA) molecules, and G-quartet/hemin (G4/H) motifs was reported by Zhang *et al.* as an electrochemical sensor for the detection of  $H_2O_2$  to mimic peroxidase-like activity.<sup>153</sup> The GO/PVA/G4/H hydrogel was synthesized *via* cation-templated self-assembly, as shown in Fig. 8a. The enzyme mimicking activity of this aerogel was revealed through the oxidation of TMB and utilized for the detection of  $H_2O_2$  (Fig. 8b). Electrodes were prepared *via* a 3D printing process on an indium tin oxide substrate (ITO) (Fig. 8c). Typical CV curves with different  $H_2O_2$  concentrations are shown in Fig. 8d, and a linear plot is shown in Fig. 8e. The detection is visualized by color change, as shown in Fig. 8f, and this can be explored for the design of bioelectronic materials with good chemical functionality.<sup>153</sup>

## 5. Applications of nano-carbon-based nanozymes

The nano-carbons-based nanozymes are the highlighted area of research because of their wide variety of applications in the field of pesticide detection, photocatalysis, sensing, biosensing, cancer treatment, wound healing, and others, as summarized in Fig. 9.<sup>19,154</sup> In the following section, we briefly describe the recent progress of nano-carbon nanozymes in diverse fields.

### 5.1. Medical aspects of nano-carbon nanozymes

The nano-carbons-based nanozymes are utilized in the biomedical field as biosensors, prodrugs, antibacterial agents, therapeutics, among other applications.<sup>22,51,155</sup> These biosensors include electrochemical sensors, immunosensors and colorimetric sensors. The different techniques, including amperometry and potentiometry, are used for the development of electrochemical sensors.<sup>111</sup> Different substrates were utilized



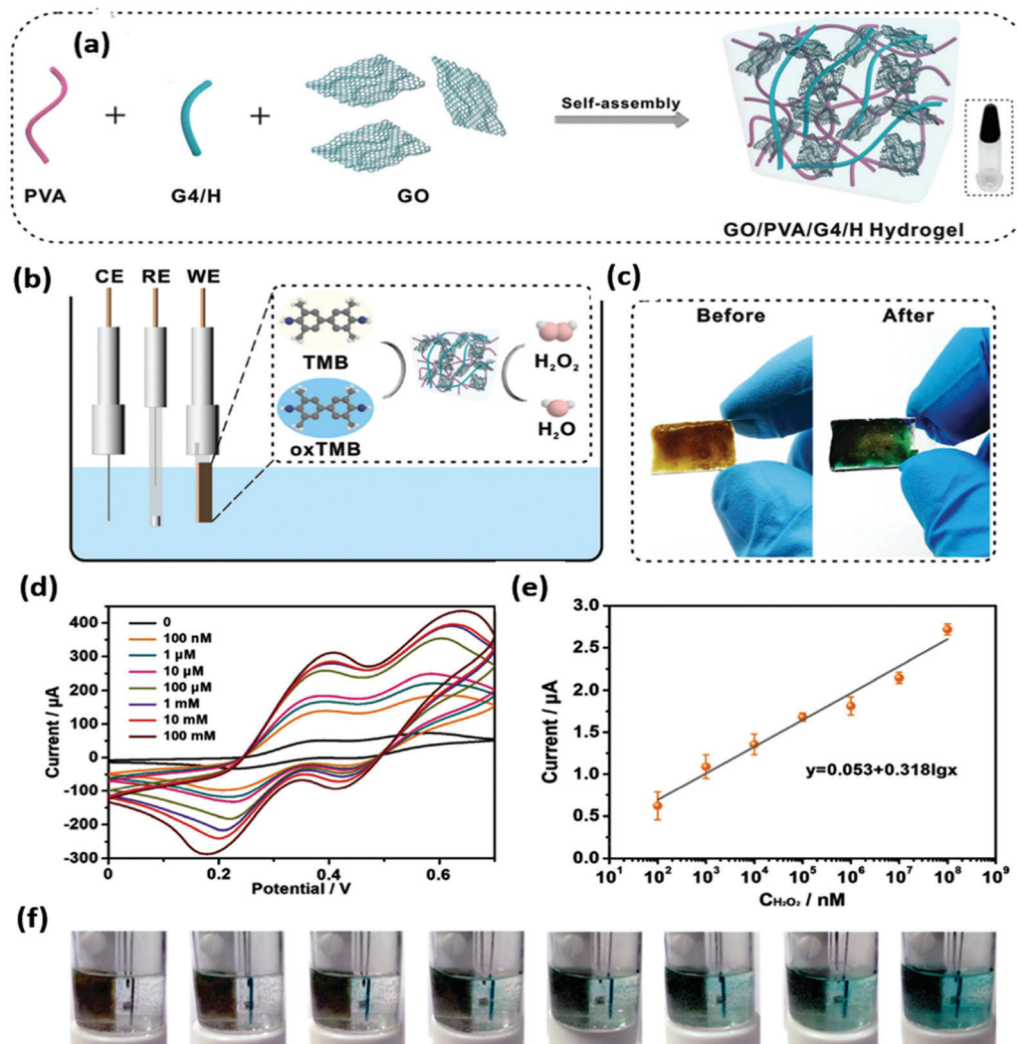


Fig. 8 (a) Schematic representation of the self-assembly of a GO/PVA/G4/H hydrogel. (b) Scheme of the GO/PVA/G4/H hydrogel as a working electrode to detect H<sub>2</sub>O<sub>2</sub>. (c) Photographs of the hydrogel before and after H<sub>2</sub>O<sub>2</sub> detection. (d) CV curves of the hydrogel. (e) The linear calibration plot for H<sub>2</sub>O<sub>2</sub> detection. (f) Photographs corresponding to the hydrogel sensor at different concentrations of H<sub>2</sub>O<sub>2</sub>.<sup>153</sup> Copyright The Royal Society of Chemistry 2020.

for the colorimetric and immune assay detection tests kits. Fungi, bacteria, and other superbugs are the major threats to world health. Many researchers are working in this line to develop anti-bacterial and antifungal treatment methods.<sup>51</sup> In the development of antibacterial substances, the properties of Gram-negative and Gram-positive bacteria need to be considered to design the efficient nanocarbon nanozyme. Habiba *et al.* have designed a silver-GQDs nanozyme to study antibacterial activity. The synthesized nanozyme was used for the antibacterial activity against *P. aeruginosa* and *S. aureus* bacteria. Silver was chosen due to its inherent antibacterial activities, and its composite with GQD incorporates water-solubility and biocompatibility. The nanozyme was PEGylated further to enhance solubility and biocompatibility. They studied the individual effect of silver NPs, pristine GQDs, and the nanocomposite nanozyme. The nanocomposite showed high antibacterial activity compared to that of pristine silver NPs and GQD. The good antibacterial activity with good cell viability

makes this nanozyme a good material for antibacterial coating and fabric design.<sup>156</sup>

Another study on bacterial infection and antibiotic-resistant treatment has been reported by Xi *et al.* The authors utilized the sponge-like morphology and peroxidase activity of the carbon nanozyme for the antibacterial activity. H<sub>2</sub>O<sub>2</sub> was used against Gram-negative bacteria (*E. coli*) and Gram-positive bacteria (*S. aureus*), along with nanozymes for the generation of ROS, which resisted the growth of bacteria by mimicking peroxidase activity.<sup>31</sup> Generally, war sites, hospitals, wounds, and others are the main areas for the bacterial infection generated from the microorganism. Gao and co-workers explored the copper-based carbon nanozyme for the destruction of the bacterial cell wall to limit bacterial infections, and utilized the oxidative states of copper supported by carbon for the antibacterial activity. The excessive ROS in the bacteria resulted in the death of the cell by POD, CAT, SOD-like activities of copper, which depends upon the oxidation state of copper.<sup>5</sup> The Fe<sub>3</sub>C/N-doped



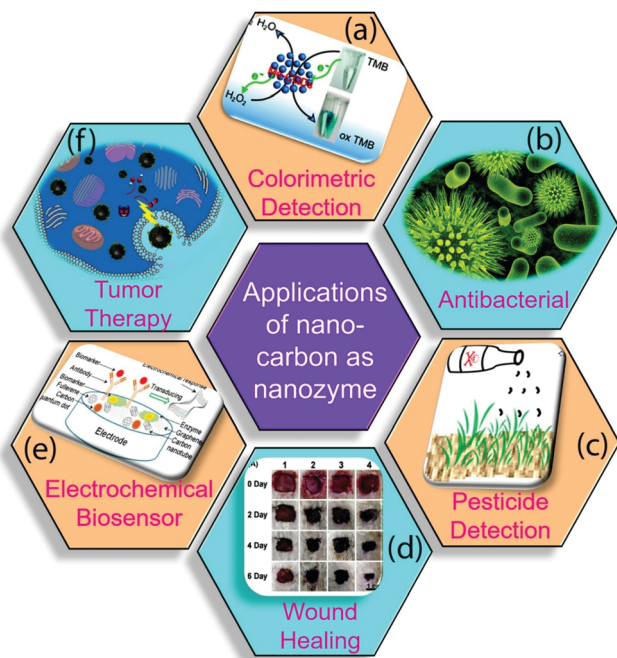


Fig. 9 Applications of nano-carbon nanozymes in various fields. (a) Colorimetric detection of cholesterol, (b) antibacterial activity, (c) detection of pesticides, (d) photographs of *S. aureus*-infected wounds, (e) tumor control, (f) electrochemical biosensor.<sup>3,4,19,83,154</sup> Copyright The American Chemical Society 2019, 2020; The Royal Society of Chemistry 2019; Elsevier Ltd. 2020.

graphitic nano-carbons were used as a broad-spectrum antimicrobial agent mimicking the peroxidase-like activity for the treatment of wound infection *in vivo*. The excellent biocompatibility and enzymatic activity were attributed to the synergistic interface effect between  $\text{Fe}_3\text{C}$  and doped-N.<sup>51</sup> Nano-carbons have been used in different biomedical applications, but their poor dispersion *in vivo* limits their activity. The surface functionalization strategy is widely used for improving their water solubility and biocompatibility.<sup>157</sup>

The electrochemical detection of biomolecules (including glucose, dopamine, uric acid and cholesterol) has been done by many research groups by using nano-carbon-based nanozymes with both ultra-high sensitivity and low detection limits.<sup>87</sup> These electrochemical detection-based tests could be useful for a clinical diagnosis, like diabetes, kidney dysfunctions, fatty liver, biomarkers detection and cancer diagnosis.<sup>158,159</sup> Wang *et al.* synthesized a gold and cobalt co-doped hollow carbon framework ( $\text{Au/Co@HNCF}$ )-based nanozyme for the electrochemical detection of uric acid. The synergy of both NPs on the carbon framework enhances the efficiency of the electrochemical sensors, and could go up to the low detection limit of  $0.023 \mu\text{M}$ . The  $\text{Au/Co@HNCF}$  biosensor shows  $\sim 1.49$ -fold higher response for uric acid oxidation than  $\text{Co@HNCF}$  because of the high electron transfer in the composite.<sup>160</sup> In an innovative approach, Li *et al.* designed CDs confined in N-doped carbon (CDs@NC) as a peroxidase-like nanozyme for the detection of gastric cancer.<sup>77</sup> The increase in the concentration

of D-proline and D-alanine was attributed to a change in metabolism as an early sign of gastric cancer. The detection of D-proline and D-alanine was done *via* visual observation of a color change with a low detection limit of  $7.7 \mu\text{M}$  for  $18.6 \mu\text{M}$ , respectively. The nanozyme activity of CDs@NC was further validated in real saliva samples.<sup>77</sup> In a similar study, the detection of cholesterol and xanthine was reported in human serum samples using Co- and N-doped CDs-based nanozymes at neutral pH.<sup>161</sup> GO was explored in the electrochemical detection of alpha-fetoprotein (AFP) and carcinoembryonic antigen (CEA) for the early detection of cancer. Feng *et al.* fabricated different composites of GO as probes for better signal detection and Au-GO composite for the signal platform. This synthesized immunosensor has high selectivity and electrochemical sensitivity for CEA and AFP.<sup>162</sup>

Landry *et al.* used the SWCNTs for the detection of proteins from *Escherichia coli* and *Pichia pastoris*.<sup>164</sup> Zhang *et al.* used functionalized SWCNT for the electrochemical detection of Microcystin-LR, and explored its application for biological immunosensors. The flower-like morphology of the SWCNTs provides a high surface area and active sites for the electrochemical detection of microcystin-LR.<sup>165</sup> The different oxidation state of copper can exhibit different enzymatic activities, *i.e.*, POD, SOD, catalase. The  $\text{Cu}^{2+}$  and  $\text{Cu}^0$ -doped hollow carbon nanospheres ( $\text{CuO-HSCs}$  and  $\text{Cu-HSCs}$ , respectively) were explored as an antibacterial agent. The investigation showed that  $\text{Cu}^{2+}$  is more effective in killing Gram-negative bacteria, but not the Gram-positive one because the cell wall of the Gram-negative bacteria is more sensitive. Meanwhile, the  $\text{Cu-HSCs}$  are effective for both bacteria. This behavior is dependent on the release of copper in the cell membrane of bacteria for easy damage and generation of ROS in the cell.<sup>4</sup> The  $\text{Fe}_3\text{C/N-C}$  nanozyme is known to catalyze the  $\text{H}_2\text{O}_2$  to form  $\bullet\text{OH}$ , which is the best remedy for the treatment of antibacterial infections. This nanozyme accelerates the formation of  $\bullet\text{OH}$  from  $\text{H}_2\text{O}_2$ , which was investigated by Gram positive (*S. aureus*) and Gram negative (*E. coli*) bacteria. In addition, the biocompatibility and safety of the nanozyme was tested on healthy rats, which showed that there was no infection or damage to the living being.<sup>51</sup>

The colorimetric method for the detection of  $\text{H}_2\text{O}_2$ , glucose, and other molecules can be explored by using nano-carbons nanozymes. N-Doped carbons, such as the peroxidase mimetic nanozyme, were synthesized from polyethylenimine (PEI) as the N precursor using the montmorillonite (MMT) template for the detection of  $\text{H}_2\text{O}_2$ , glucose, and ascorbic acid as shown in Fig. 10.<sup>163</sup> Ren *et al.* conducted the colorimetric detection of glucose by synthesizing a cost-effective molybdenum oxide carbon nanozyme with nanorod morphology. The investigation revealed that the nanozyme exhibited peroxidase-like activity, and could detect glucose up to a low detection (LOD) limit of  $0.181 \mu\text{M}$ .<sup>166</sup> A similar report has been given by Honarasa and co-workers on the nanomolar detection of  $\text{H}_2\text{O}_2$ , where nano-carbons supported  $\text{Fe}_3\text{O}_4$  was used as a catalyst.<sup>167</sup> Fe-doped CDs were also used for the detection of serum glucose in mice with a detection limit of  $5 \mu\text{M}$ . The author explored its magnetic property for bioimaging in MRI, and checked the biocompatibility with U87MG and HepG2 cells.<sup>168</sup> Li *et al.*



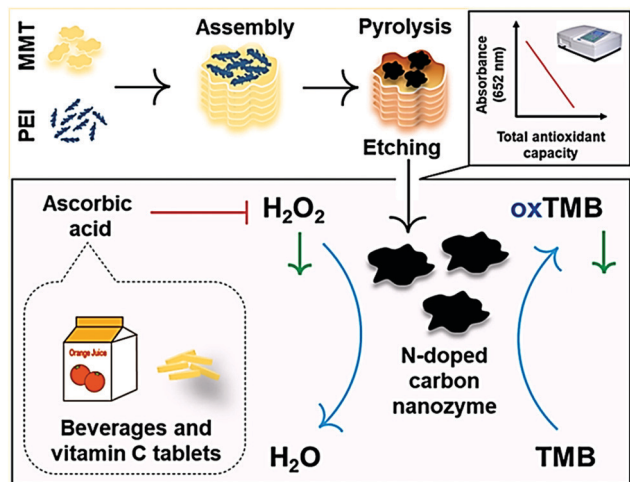


Fig. 10 N-Doped carbon as a peroxidase-like catalyst for the detection of  $H_2O_2$ , glucose, and ascorbic acid.<sup>163</sup> Copyright American Chemical Society 2019.

studied the effect of  $Fe_3C/N$ -doped graphitic carbon on the wound healing treatment. This nanozyme decomposes  $H_2O_2$  into the  $HO^\bullet$ -radical, resulting in excessive ROS that leads to antibacterial activity, which accelerates wound healing.<sup>37</sup>

Photodynamic therapy (PDT) is used for the treatment of cancer and other diseases. Xu *et al.* synthesized the HCS@Pt-chlorin e6 (Ce6) composite-based nanozyme as a

PDT agent and peroxidase to increase the ROS concentration for cancer treatment.<sup>19</sup> Wang *et al.* designed nano-carbons supported ultrafine  $Mo_2C@MoOx$  nanoclusters ( $C/Mo_2C@MoOx$ ) as an oxidase mimic, starting with the Mo/ZIF-8 MOF precursor for the photothermal tumor therapy. The catalytic mechanism involves absorption of NIR light, generation of cytotoxic heat, and the regulation of ROS generation activity.<sup>169</sup> Sun *et al.* investigated the underlying mechanism of peroxidase-like activity and protective effect of GOQDs toward the acceleration of alcohol metabolism and treatment of alcoholic liver disease. GOQDs were found to decrease mitochondrial damage and ROS generation. Furthermore, autophagy was slightly increased, which helped in the removal of accumulated lipids (Fig. 11). The viability of the cell and membrane integrity was also tested with GOQDs against ethanol, and it was concluded that the nano-catalyst inverted the effect of alcohol by 80%.<sup>136</sup> The catalase-like activity of nanozymes was also explored for photothermal and photodynamic therapy to relieve tumor hypoxia. In a typical example by Yang *et al.*, platinum-based carbon was investigated for tumor inhibition *in vivo* by the combination of the photothermal/photodynamic properties of platinum and carbon. The enhanced catalase-like activity favors the decomposition of endogenous  $H_2O_2$  and controlled ROS generation, which in consequence, improves the effects of photodynamic therapy.<sup>170</sup> In addition to photodynamic therapy, sonodynamic therapy/sonosensitizers was investigated for the mitigation of tumor.<sup>171</sup> Sonodynamic

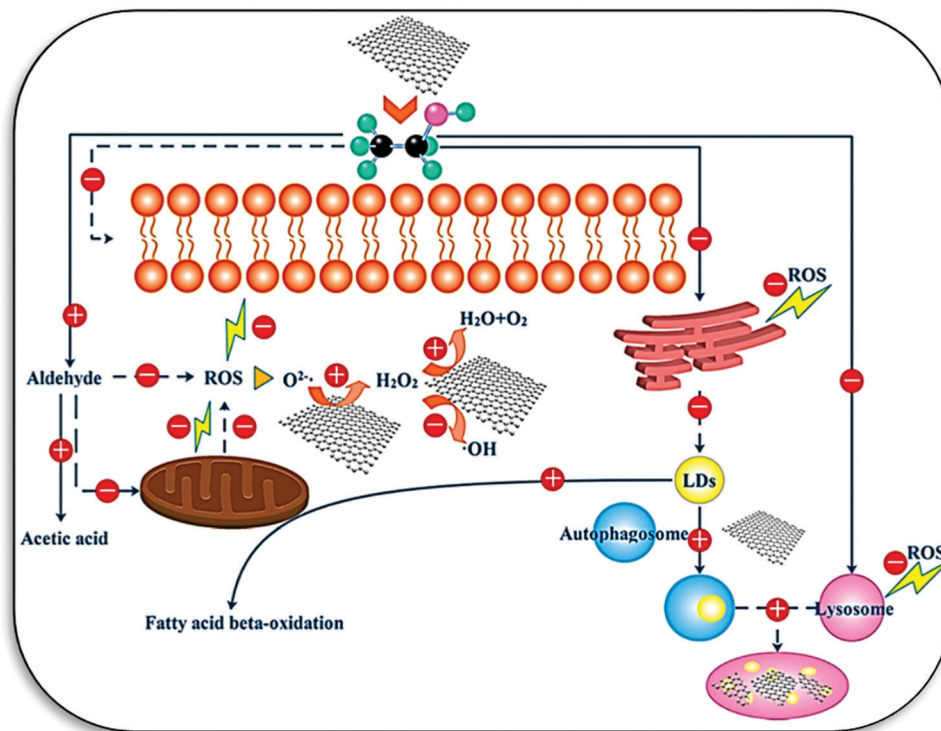


Fig. 11 Mechanisms underlying the detoxification effects of GOQDs on ethanol-induced cytotoxicity (LDs, lipid droplets). The plus and minus signs indicate the up and down regulation of the corresponding biological responses, respectively. The solid and dashed lines illustrate the direct and indirect effects of GOQDs on the cellular components or bioprocesses, respectively.<sup>136</sup> Copyright American Chemical Society 2017.



therapy exhibits an advantage over photodynamic therapy owing to its deeper tissue penetration depth and low cost. However, the low photothermal conversion and low sonosensitization efficacy of nano-carbon nanozymes are still significant challenges for real life adaptability.

## 5.2. Environmental aspects of nano-carbon nanozymes

The growing population and increase in rapid industrialization and modernization have put human health at risk. The release of poisonous gases and wastewater either without or inefficient treatments makes an unhealthy environment for mankind.<sup>20,21,172–174</sup> The release of heavy metals like chromium, mercury, arsenic, lead, cadmium, dyes, pharma waste, and others has gathered the attention of researchers. To resolve the issue of wastewater treatment, many adsorptions, degradation methods, and catalysts were evolved during the past two decades. However, the nano-carbon nanozyme exhibits significant potential among all available techniques because of their natural enzyme-mimicking properties. Wang *et al.* synthesized Au-doped thiol graphene as a sensing platform for the detection of mercury, where the zirconia-based MOF is used as a nanozyme for enhancing the signal for the detection.<sup>175</sup> The pesticide detection and their photodegradation have been reported by Das and co-workers by using Fe<sub>3</sub>O<sub>4</sub>-TiO<sub>2</sub>-graphene as a nanozyme. The graphene interacts with the organic pollutants with its  $\pi$  electron cloud and the  $\pi$ - $\pi$  interaction leads to the adsorption and degradation of pesticides. TiO<sub>2</sub> reduces the bandgap and caps the excited photoelectron for the degradation, while Fe<sub>3</sub>O<sub>4</sub> has peroxidase-like activity. The designed nanocomposite has shown colorimetric detection by oxidizing the peroxidase substrate TMB, which has changed its color to

blue (Fig. 12).<sup>176</sup> Organophosphate compounds are one of the organic pollutants used in many pesticides. Wei *et al.* utilized nanoceria for the detection of organophosphate compounds (OPC), as nanoceria has phosphatase mimicking properties and CDs have been used to enhance the catalytic properties.<sup>177</sup>

The single-atom iron was used as a nanozyme in combination with N-doped graphene to explore the peroxidase mimicking activity. The colorimetric detection method was explored, where the TMB is oxidized, and this nanozyme could go up to the low detection limit of chromium, *i.e.*, 3 nM.<sup>178</sup> Another report showed the detection of fluoride in water using graphitic carbon nitride quantum dots (g-CNQDs) as a nanozyme with the low detection limit of 4.06  $\mu$ M. The efficient detection of fluoride is because of the interaction between fluorine electrons and  $\pi$ -electrons of g-CNQDs and surface functional groups.<sup>179</sup> The colorimetric detection of mercury is shown by Mohammadpour *et al.*, who used CNDs to fabricate the on and off sensors.<sup>180</sup> The detection of ascorbic acid (AA) was investigated by Chandra *et al.* AA is an important nutrient used in different foods and pharmaceutical industries. The mustard seeds-derived CQDs have been used for the colorimetric detection of AA.<sup>181</sup>

Para nitrophenol (PNP) is one of the dangerous organic effluents, which can cause kidney and liver damage. Qiu *et al.* have developed a colorimetric sensor for the detection of PNP. The 3D nano-carbon-based nanozyme has been designed with mesoporous Fe<sub>3</sub>O<sub>4</sub>, which is known to show peroxidase-like activity. The  $\pi$ - $\pi$  interaction of the graphene-based nanohybrid for detection could go up to the low detection limit of PNP with high sensitivity and selectivity.<sup>146</sup> The dye degradation ability of graphene-Au NPs synthesized by a simple hydrothermal

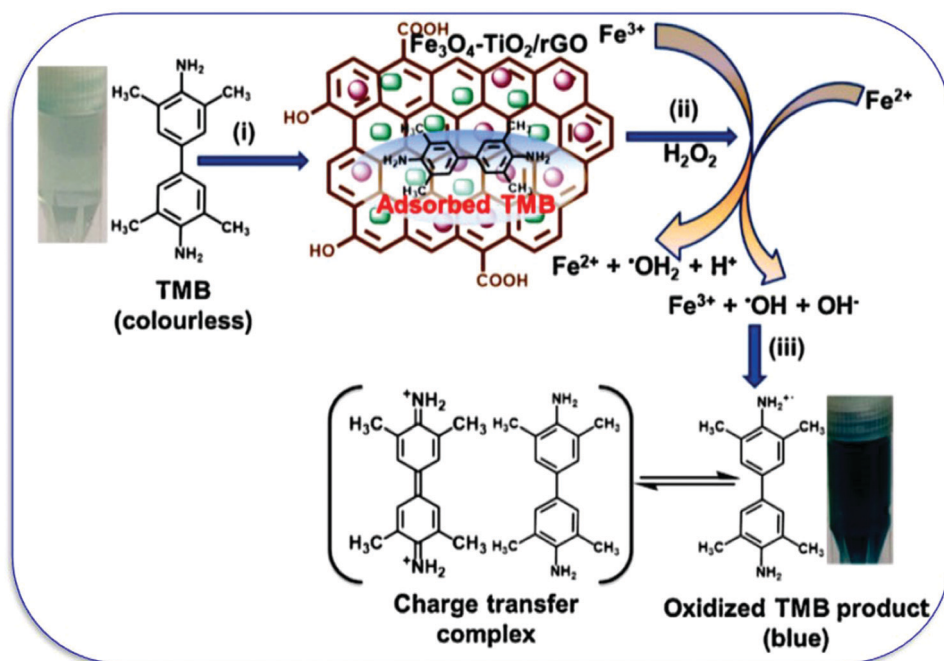


Fig. 12 The peroxidase-like activity of the FTG nanocomposite showing the (i) adsorption of TMB onto the FTG nanocomposite surface, (ii) formation of •OH by the Fenton reaction, and (iii) TMB oxidation by •OH radicals.<sup>176</sup> Copyright Elsevier B.V. 2019.





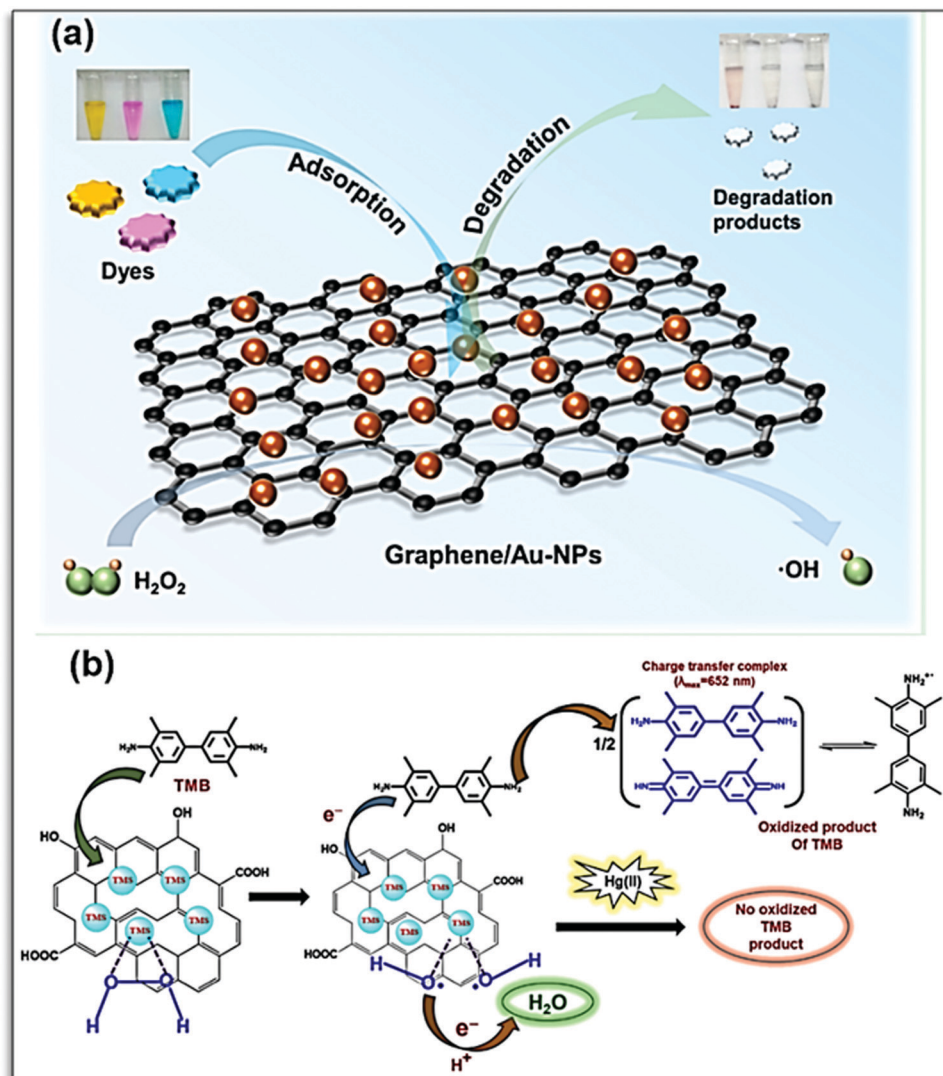


Fig. 13 (a) Schematic representation of the peroxidase-mimicking activity of graphene/Au-NPs for the adsorption and degradation of dyes.<sup>182</sup> (b) Mechanism of peroxidase-mimicking activity of transition metal sulfide (TMS)/p-rGO nanocomposites in the presence and absence of Hg(II) ions.<sup>183</sup> Copyright American Chemical Society 2021.

method has been reported by Li *et al.* Incorporation of Au NPs enhances the catalytic activity of graphene, which exhibits excellent molecular binding ability toward dyes. The dyes were removed by the synergistic effect of adsorption and degradation, where OH plays a crucial role, as shown in Fig. 13a.<sup>182</sup> This nanocomposite shows that the catalytic mechanism similar to natural peroxidase relies on substrate binding on active sites. Incorporation of CuS and NiS on rGO enhances the substrate binding affinity of transition metal sulfide (TMS)/p-rGO nanocomposites towards Hg(II) due to the strong interaction between Hg-S. A TMS/p-rGO-based paper strip colorimetric sensor can detect Hg(II) with a lower limit of detection at 50 nM.<sup>183</sup> The presence of Hg(II) blocks the active site of TMS/p-rGO and limits its catalytic activity, as shown in Fig. 13b, which can be visualized by color change.<sup>183</sup> The release of pharma waste in the water is another important issue to resolve. Their contamination in the environment of

aquatic animals can lead to a major threat as many aquatic animals are consumed by humans, which leads to health disorders. To address this issue, many researchers have done extensive work. Borthakur *et al.* utilized the peroxidase activity of g-C<sub>3</sub>N<sub>4</sub> and h-BN nanocomposite decorated with CuS nanoparticles. Both synthesized nanozymes showed significant TMB oxidation, and this property was utilized for the sensing of the Ibrufen (Ibu) molecules. The Ibu molecules show  $\pi$ - $\pi$  interaction and are adsorbed on the surface of the catalyst with the functionality present on the surface, hence leading to the poor interaction of the catalyst with TMB. Thus, the poor interaction inhibits the peroxidase activity and enhances the detection of Ibu.<sup>184</sup>

## 6. Conclusion

Nano-carbons have emerged as a promising material for enzyme mimetics with excellent biocompatibility and remarkable



performance in biopharmaceuticals, clinical medicine, environmental management, and molecular detection. The structure and properties of nano-carbons, including size, shape, surface lattice, surface functionalization, and composition, have a strong impact on their catalytic activity. Nanozymes with a high surface-to-volume ratio, high density of dangling bonds and active sites, and accelerated electron transfer show enhanced sensitivity and selectivity. The nanozyme research is highly dynamic with numerous opportunities and exciting challenges. This review intended to highlight the current advances of nano-carbons as enzyme mimetic catalysts and their applications for different catalysis reactions. Despite major advances achieved for nano-carbons in enzyme mimetics, the nanozymes research and applications are still full of challenges to be overcome. It is always a persistent goal to synthesize nanozymes with outstanding catalytic activity and ultra-selectivity. In addition, the majority of the work only describes the synthesis and utilization of nano-carbons in different enzymatic activities without paying much attention to the underlying mechanism and catalytic turnover. For future nanozyme research, a comprehensive study of the mechanism can help the fabrication of precise and highly efficient nanozymes.

It remains a challenge to synthesize and design a nano-carbon, which simultaneously fulfills the requirement of ultra-sensitivity, selectivity, and cost-effectiveness since the active sites of nanozymes are quite different from that of a protein-based enzyme. For the successful application of nanozymes in the biomedical and agriculture fields, the interaction between plant/animal cells and nanozymes is crucial to study. Future applications of nanozymes as biomedicine strongly depend on their biosafety and biocompatibility, which is a big challenge to overcome with high selectivity and precision. Little is known about the influences of nano-carbon nanozymes toward the endogenous antioxidant defense-associated metabolites. Future perspectives in this direction can involve the fate of nanozymes and every step of treatment, distribution, accumulation, and metabolism, along with their toxicity.

## Conflicts of interest

The authors declare no conflict of interest.

## Acknowledgements

K. M. T. acknowledges financial assistance from the Department of Biotechnology (DBT), India, through the Ramalingaswami Faculty Award (BT/RLF/Re-entry/45/2018).

## References

- X. Li, X. Wu, T. Yuan, J. Zhu and Y. Yang, *Biochem. Eng. J.*, 2021, **175**, 108139.
- M. Liang and X. Yan, *Acc. Chem. Res.*, 2019, **52**, 2190–2200.
- L. Zhao, Z. Wu, G. Liu, H. Lu, Y. Gao, F. Liu, C. Wang, J. Cui and G. Lu, *J. Mater. Chem. B*, 2019, **7**, 7042–7051.
- J. Xi, G. Wei, L. An, Z. Xu, Z. Xu, L. Fan and L. Gao, *Nano Lett.*, 2019, **19**, 7645–7654.
- J. Zhang, Y. Lin, S. Wu, X. Hou, C. Zheng, P. Wu and J. Liu, *Carbon*, 2021, **182**, 537–544.
- F. Li, Q. Chang, N. Li, C. Xue, H. Liu, J. Yang, S. Hu and H. J. C. E. J. Wang, *Chem. Eng. J.*, 2020, **394**, 125045.
- L. Zhao, X. Ren, J. Zhang, W. Zhang, X. Chen and X. Meng, *New J. Chem.*, 2020, **44**, 1988–1992.
- H. Sun, Y. Zhou, J. Ren and X. Qu, *Angew. Chem., Int. Ed.*, 2018, **57**, 9224–9237.
- H. Wei, L. Gao, K. Fan, J. Liu, J. He, X. Qu, S. Dong, E. Wang and X. Yan, *Nano Today*, 2021, **40**, 101269.
- S. Tanaka, Y. V. Kaneti, R. Bhattacharjee, M. N. Islam, R. Nakahata, N. Abdullah, S.-I. Yusa, N.-T. Nguyen, M. J. A. Shiddiky, Y. Yamauchi and M. S. A. Hossain, *ACS Appl. Mater. Interfaces*, 2018, **10**, 1039–1049.
- B. Liu, Y. Wang, Y. Chen, L. Guo and G. Wei, *J. Mater. Chem. B*, 2020, **8**, 10065–10086.
- N. Baig, I. Kammakakam and W. Falath, *Mater. Adv.*, 2021, **2**, 1821–1871.
- K. Boriachek, M. K. Masud, C. Palma, H.-P. Phan, Y. Yamauchi, M. S. A. Hossain, N.-T. Nguyen, C. Salomon and M. J. A. Shiddiky, *Anal. Chem.*, 2019, **91**, 3827–3834.
- X. Wang, H. Wang and S. Zhou, *J. Phys. Chem. Lett.*, 2021, **12**, 11751–11760.
- F. Manea, F. B. Houillon, L. Pasquato and P. Scrimin, *Angew. Chem., Int. Ed.*, 2004, **43**, 6165–6169.
- L. Gao, J. Zhuang, L. Nie, J. Zhang, Y. Zhang, N. Gu, T. Wang, J. Feng, D. Yang, S. Perrett and X. Yan, *Nat. Nanotechnol.*, 2007, **2**, 577–583.
- P. Wang, T. Wang, J. Hong, X. Yan and M. Liang, *Front. Bioeng. Biotechnol.*, 2020, **8**, 15.
- R. Zhang, K. Fan and X. Yan, *Sci. China: Life Sci.*, 2020, **63**, 1183–1200.
- Z. Xu, P. Sun, J. Zhang, X. Lu, L. Fan, J. Xi, J. Han and R. Guo, *Chem. Eng. J.*, 2020, **399**, 125797.
- C. A. S. Ballesteros, L. A. Mercante, A. D. Alvarenga, M. H. M. Facure, R. Schneider and D. S. Correa, *Mater. Chem. Front.*, 2021, **5**, 7419–7451.
- W. Chen, S. Li, J. Wang, K. Sun and Y. Si, *Nanoscale*, 2019, **11**, 15783–15793.
- D. Jiang, D. Ni, Z. T. Rosenkrans, P. Huang, X. Yan and W. Cai, *Chem. Soc. Rev.*, 2019, **48**, 3683–3704.
- Y. Meng, W. Li, X. Pan and G. M. Gadd, *Environ. Sci.: Nano*, 2020, **7**, 1305–1318.
- M. K. Masud, J. Na, M. Younus, M. S. A. Hossain, Y. Bando, M. J. A. Shiddiky and Y. Yamauchi, *Chem. Soc. Rev.*, 2019, **48**, 5717–5751.
- R. Zhang, X. Yan and K. Fan, *Acc. Mater. Res.*, 2021, **2**, 534–547.
- D. He, M. Yan, P. Sun, Y. Sun, L. Qu and Z. Li, *Chin. Chem. Lett.*, 2021, **32**, 2994–3006.
- X. Huang, S. Zhang, Y. Tang, X. Zhang, Y. Bai and H. Pang, *Coord. Chem. Rev.*, 2021, **449**, 214216.
- P. Zhang, D. Sun, A. Cho, S. Weon, S. Lee, J. Lee, J. W. Han, D.-P. Kim and W. Choi, *Nat. Commun.*, 2019, **10**, 940.



- 29 S. Sahani, K. Malika Tripathi, T. Il Lee, D. P. Dubal, C.-P. Wong, Y. Chandra Sharma and T. Young Kim, *Energy Convers. Manage*, 2022, **252**, 115133.
- 30 A. Sharma, R. K. Sharma, Y.-K. Kim, H.-J. Lee and K. M. Tripathi, *J. Environ. Chem. Eng.*, 2021, **9**, 106656.
- 31 P. Kumari, K. M. Tripathi, L. K. Jangir, R. Gupta and K. Awasthi, *Mater. Today Chem.*, 2021, **22**, 100597.
- 32 H. Wang, S.-T. Yang, A. Cao and Y. Liu, *Acc. Chem. Res.*, 2013, **46**, 750–760.
- 33 Y. Morimoto, M. Horie, N. Kobayashi, N. Shinohara and M. Shimada, *Acc. Chem. Res.*, 2013, **46**, 770–781.
- 34 K. M. Tripathi, A. Bhati, A. Singh, A. K. Sonker, S. Sarkar and S. K. Sonkar, *ACS Sustainable Chem. Eng.*, 2017, **5**, 2906–2916.
- 35 A. Bhati, Gunture, K. M. Tripathi, A. Singh, S. Sarkar and S. K. Sonkar, *New J. Chem.*, 2018, **42**, 16411–16427.
- 36 V. K. Bajpai, S. Shukla, I. Khan, S.-M. Kang, Y. Haldorai, K. M. Tripathi, S. Jung, L. Chen, T. Kim, Y. S. Huh and Y.-K. Han, *ACS Appl. Mater. Interfaces*, 2019, **11**, 43949–43963.
- 37 A. Sharma, N. Sharma, A. Kumari, H.-J. Lee, T. Kim and K. M. Tripathi, *Appl. Mater. Today*, 2020, **18**, 100467.
- 38 S. K. Sonkar, K. M. Tripathi and S. Sarkar, *J. Nanosci. Nanotechnol.*, 2014, **14**, 2532–2538.
- 39 H. Wang, K. Wan and X. Shi, *Adv. Mater.*, 2019, **31**, 1805368.
- 40 A. S. Jalilov, L. G. Nilewski, V. Berka, C. Zhang, A. A. Yakovenko, G. Wu, T. A. Kent, A.-L. Tsai and J. M. Tour, *ACS Nano*, 2017, **11**, 2024–2032.
- 41 E. L. G. Samuel, D. C. Marcano, V. Berka, B. R. Bitner, G. Wu, A. Potter, R. H. Fabian, R. G. Pautler, T. A. Kent, A.-L. Tsai and J. M. Tour, *Proc. Natl. Acad. Sci. U. S. A.*, 2015, **112**, 2343–2348.
- 42 M. Zandieh and J. Liu, *ACS Nano*, 2021, **15**, 15645–15655.
- 43 H. Wang, M. Zhang, K. Wei, Y. Zhao, H. Nie, Y. Ma, Y. Zhou, H. Huang, Y. Liu, M. Shao and Z. Kang, *Carbon*, 2021, **179**, 692–700.
- 44 G. Wu, E. A. McHugh, V. Berka, W. Chen, Z. Wang, J. L. Beckham, P. J. Derry, T. Roy, T. A. Kent, J. M. Tour and A.-L. Tsai, *ACS Appl. Nano Mater.*, 2020, **3**, 6962–6971.
- 45 R. Bhattacharjee, S. Tanaka, S. Moriam, M. K. Masud, J. Lin, S. M. Alshehri, T. Ahamad, R. R. Salunkhe, N.-T. Nguyen, Y. Yamauchi, M. S. A. Hossain and M. J. A. Shiddiky, *J. Mater. Chem. B*, 2018, **6**, 4783–4791.
- 46 V. K. Bajpai, I. Khan, S. Shukla, S.-M. Kang, F. Aziz, K. M. Tripathi, D. Saini, H.-J. Cho, N. Su Heo, S. K. Sonkar, L. Chen, Y. Suk Huh and Y.-K. Han, *Theranostics*, 2020, **10**, 7841–7856.
- 47 C. Ren, X. Hu and Q. Zhou, *Adv. Sci.*, 2018, **5**, 1700595.
- 48 S. Tanaka, M. K. Masud, Y. V. Kaneti, M. J. A. Shiddiky, A. Fatehmulla, A. M. Aldhafiri, W. A. Farooq, Y. Bando, M. S. A. Hossain and Y. Yamauchi, *ChemNanoMat*, 2019, **5**, 506–513.
- 49 M. K. Masud, J. Kim, M. M. Billah, K. Wood, M. J. A. Shiddiky, N.-T. Nguyen, R. K. Parsapur, Y. V. Kaneti, A. A. Alshehri, Y. G. Alghamidi, K. A. Alzahrani, M. Adharvanachari, P. Selvam, M. S. A. Hossain and Y. Yamauchi, *J. Mater. Chem. B*, 2019, **7**, 5412–5422.
- 50 M. K. Masud, S. Yadav, M. N. Islam, N.-T. Nguyen, C. Salomon, R. Kline, H. R. Alamri, Z. A. Allothman, Y. Yamauchi, M. S. A. Hossain and M. J. A. Shiddiky, *Anal. Chem.*, 2017, **89**, 11005–11013.
- 51 Y. Li, W. Ma, J. Sun, M. Lin, Y. Niu, X. Yang and Y. Xu, *Carbon*, 2020, **159**, 149–160.
- 52 J. Zhang, X. Lu, D. Tang, S. Wu, X. Hou, J. Liu and P. Wu, *ACS Appl. Mater. Interfaces*, 2018, **10**, 40808–40814.
- 53 G. Wu, V. Berka, P. J. Derry, K. Mendoza, E. Kakadiaris, T. Roy, T. A. Kent, J. M. Tour and A.-L. Tsai, *ACS Nano*, 2019, **13**, 11203–11213.
- 54 K. M. Tripathi, H. T. Ahn, M. Chung, X. A. Le, D. Saini, A. Bhati, S. K. Sonkar, M. I. Kim and T. Kim, *ACS Biomater. Sci. Eng.*, 2020, **6**, 5527–5537.
- 55 V. K. Singh, P. K. Yadav, S. Chandra, D. Bano, M. Talat and S. H. Hasan, *J. Mater. Chem. B*, 2018, **6**, 5256–5268.
- 56 R. Zhang, L. Chen, Q. Liang, J. Xi, H. Zhao, Y. Jin, X. Gao, X. Yan, L. Gao and K. Fan, *Nano Today*, 2021, **41**, 101317.
- 57 F. Meng, M. Peng, Y. Chen, X. Cai, F. Huang, L. Yang, X. Liu, T. Li, X. Wen, N. Wang, D. Xiao, H. Jiang, L. Xia, H. Liu and D. Ma, *Appl. Catal., B*, 2022, **301**, 120826.
- 58 S. K. Tiwari, R. Pandey, N. Wang, V. Kumar, O. J. Sunday, M. Bystrzejewski, Y. Zhu and Y. K. Mishra, *Adv. Sci.*, 2022, 2105770.
- 59 Á. Serrano-Aroca, K. Takayama, A. Tuñón-Molina, M. Seyran, S. S. Hassan, P. Pal Choudhury, V. N. Uversky, K. Lundstrom, P. Adadi, G. Palù, A. A. A. Aljabali, G. Chauhan, R. Kandimalla, M. M. Tambuwala, A. Lal, T. M. Abd El-Aziz, S. Sherchan, D. Barh, E. M. Redwan, N. G. Bazan, Y. K. Mishra, B. D. Uhal and A. Brufsky, *ACS Nano*, 2021, **15**, 8069–8086.
- 60 S. K. Bhardwaj, M. Mujawar, Y. K. Mishra, N. Hickman, M. Chavali and A. Kaushik, *Nanotechnology*, 2021, **32**, 502001.
- 61 S. Luo, M. Sha, F. Tian, X. Li, L. Fu, Y. Gu, L.-L. Qu, G.-H. Yang and C. Zhu, *Chin. Chem. Lett.*, 2022, **33**, 344–348.
- 62 N. Dhiman, D. Pradhan and P. Mohanty, *Fuel*, 2021, 122722, DOI: 10.1016/j.fuel.2021.122722.
- 63 N. Dhiman and P. Mohanty, *New J. Chem.*, 2019, **43**, 16670–16675.
- 64 A. Muhulet, F. Miculescu, S. I. Voicu, F. Schütt, V. K. Thakur and Y. K. Mishra, *Mater. Today Energy*, 2018, **9**, 154–186.
- 65 G. S. Das, A. Bhatnagar, P. Yli-Pirilä, K. M. Tripathi and T. Kim, *Chem. Commun.*, 2020, **56**, 6953–6956.
- 66 D. Huang, Y. Chen, M. Cheng, L. Lei, S. Chen, W. Wang and X. Liu, *Small*, 2021, **17**, 2002998.
- 67 X. Bi, Q. Bai, L. Wang, F. Du, M. Liu, W. W. Yu, S. Li, J. Li, Z. Zhu, N. Sui and J. Zhang, *Nano Res.*, 2022, **15**, 1446–1454.
- 68 L. Jiao, W. Xu, Y. Zhang, Y. Wu, W. Gu, X. Ge, B. Chen, C. Zhu and S. Guo, *Nano Today*, 2020, **35**, 100971.
- 69 J. Gao, L. Zhang, Y. Tang, Q. Qin and C. Wu, *Anal. Chim. Acta*, 2020, **1138**, 158–167.
- 70 K. Fan, J. Xi, L. Fan, P. Wang, C. Zhu, Y. Tang, X. Xu, M. Liang, B. Jiang, X. Yan and L. Gao, *Nat. Commun.*, 2018, **9**, 1440.



- 71 W. Zhu, N. Hao, J. Lu, Z. Dai, J. Qian, X. Yang and K. Wang, *Chem. Commun.*, 2020, **56**, 1409–1412.
- 72 Y. Hu, X. J. Gao, Y. Zhu, F. Muhammad, S. Tan, W. Cao, S. Lin, Z. Jin, X. Gao and H. Wei, *Chem. Mater.*, 2018, **30**, 6431–6439.
- 73 H. Yang, J. Xiao, L. Su, T. Feng, Q. Lv and X. Zhang, *Chem. Commun.*, 2017, **53**, 3882–3885.
- 74 S. Li, X. Zhao, R. Gang, B. Cao and H. Wang, *Anal. Chem.*, 2020, **92**, 5152–5157.
- 75 K. Wu, Y. Feng, Y. Li, L. Li, R. Liu and L. Zhu, *Anal. Bioanal. Chem.*, 2020, **412**, 5477–5487.
- 76 S. Hu, W. Zhang, N. Li, Q. Chang and J. J. A. S. S. Yang, *Appl. Surf. Sci.*, 2021, **545**, 148987.
- 77 Z. Li, W. Liu, P. Ni, C. Zhang, B. Wang, G. Duan, C. Chen, Y. Jiang and Y. Lu, *Chem. Eng. J.*, 2022, **428**, 131396.
- 78 Y. Zhan, S. Yang, F. Luo, L. Guo, Y. Zeng, B. Qiu and Z. Lin, *ACS Appl. Mater. Interfaces*, 2020, **12**, 30085–30094.
- 79 S. Polepalli, B. Uttam and C. P. Rao, *Mater. Adv.*, 2020, **1**, 2074–2083.
- 80 N. Chakraborty, D. Jha, H. K. Gautam and I. Roy, *Mater. Adv.*, 2020, **1**, 774–782.
- 81 X. Ruan, D. Liu, X. Niu, Y. Wang, C. D. Simpson, N. Cheng, D. Du and Y. Lin, *Anal. Chem.*, 2019, **91**, 13847–13854.
- 82 J. Xi, G. Wei, Q. Wu, Z. Xu, Y. Liu, J. Han, L. Fan and L. Gao, *Biomater. Sci.*, 2019, **7**, 4131–4141.
- 83 Y. Zhu, J. Wu, L. Han, X. Wang, W. Li, H. Guo and H. Wei, *Anal. Chem.*, 2020, **92**, 7444–7452.
- 84 S. Lin, Y. Zhang, W. Cao, X. Wang, L. Qin, M. Zhou and H. Wei, *Dalton Trans.*, 2019, **48**, 1993–1999.
- 85 Q. Liang, J. Xi, X. J. Gao, R. Zhang, Y. Yang, X. Gao, X. Yan, L. Gao and K. Fan, *Nano Today*, 2020, **35**, 100935.
- 86 J. Wu, W. Lv, Q. Yang, H. Li and F. Li, *Biosens. Bioelectron.*, 2021, **171**, 112707.
- 87 D. Saini, Gunture, J. Kaushik, R. Aggarwal, K. M. Tripathi and S. K. Sonkar, *ACS Appl. Nano Mater.*, 2021, **4**, 12825–12844.
- 88 C. Dalal, D. Saini, A. K. Garg and S. K. Sonkar, *ACS Appl. Bio Mater.*, 2021, **4**, 252–266.
- 89 A. Aijaz, J. Masa, C. Rösler, H. Antoni, R. A. Fischer, W. Schuhmann and M. Muhler, *Chem. – Eur. J.*, 2017, **23**, 12125–12130.
- 90 S. He, J. Huang, Q. Zhang, W. Zhao, Z. Xu and W. Zhang, *Adv. Funct. Mater.*, 2021, **31**, 2105198.
- 91 J. Jin, W. Song, J. Wang, L. Li, Y. Tian, S. Zhu, Y. Zhang, S. Xu, B. Yang and B. Zhao, *Chem. Eng. J.*, 2022, **430**, 132687.
- 92 L. Lin, H. Ma, C. Yang, W. Chen, S. Zeng and Y. Hu, *Mater. Adv.*, 2020, **1**, 2789–2796.
- 93 H. Dong, Y. Fan, W. Zhang, N. Gu and Y. Zhang, *Bioconjugate Chem.*, 2019, **30**, 1273–1296.
- 94 X. Jiang, K. Liu, Q. Li, M. Liu, M. Yang and X. Chen, *Chem. Commun.*, 2021, **57**, 1623–1626.
- 95 Y. Sheng, Y. Zhu, M. L. Cerón, Y. Yi, P. Liu, P. Wang, T. Xue, M. B. Camarada and Y. Wen, *J. Electroanal. Chem.*, 2021, **895**, 115522.
- 96 B. Liu and J. Liu, *Nano Res.*, 2017, **10**, 1125–1148.
- 97 G. Tang, J. He, J. Liu, X. Yan and K. Fan, *Exploration*, 2021, **1**, 75–89.
- 98 Z. Wang, R. Zhang, X. Yan and K. Fan, *Mater. Today*, 2020, **41**, 81–119.
- 99 G. S. Das, K. M. Tripathi, G. Kumar, S. Paul, S. Mehara, S. Bhowmik, B. Pakhira, S. Sarkar, M. Roy and T. Kim, *New J. Chem.*, 2019, **43**, 14575–14583.
- 100 J. Kaushik, Himanshi, V. Kumar, K. M. Tripathi and S. K. Sonkar, *Chemosphere*, 2022, **287**, 132225.
- 101 J. Kaushik, Gunture, K. M. Tripathi, R. Singh and S. K. Sonkar, *Chemosphere*, 2022, **287**, 132105.
- 102 H. Sun, A. Zhao, N. Gao, K. Li, J. Ren and X. Qu, *Angew. Chem., Int. Ed.*, 2015, **54**, 7176–7180.
- 103 A.-X. Zheng, Z.-X. Cong, J.-R. Wang, J. Li, H.-H. Yang and G.-N. Chen, *Biosens. Bioelectron.*, 2013, **49**, 519–524.
- 104 Y. Song, K. Qu, C. Zhao, J. Ren and X. Qu, *Adv. Mater.*, 2010, **22**, 2206–2210.
- 105 R. T. P. da Silva, M. P. de Souza Rodrigues, G. F. B. Davilla, A. M. R. P. da Silva, A. H. B. Dourado and S. I. Córdoba de Torresi, *ACS Appl. Nano Mater.*, 2021, **4**, 12062–12072.
- 106 L. Fan, X. Xu, C. Zhu, J. Han, L. Gao, J. Xi and R. Guo, *ACS Appl. Mater. Interfaces*, 2018, **10**, 4502–4511.
- 107 D.-B. Xiong, M. Cao, Q. Guo, Z. Tan, G. Fan, Z. Li and D. Zhang, *ACS Nano*, 2015, **9**, 6934–6943.
- 108 Y. Xu, D. Li, M. Liu, F. Niu, J. Liu and E. Wang, *Sci. Rep.*, 2017, **7**, 4499.
- 109 L. Zhang, P. Wang, W. Zheng and X. Jiang, *J. Mater. Chem. B*, 2017, **5**, 6601–6607.
- 110 H. E. Lim, Y. Miyata, R. Kitaura, Y. Nishimura, Y. Nishimoto, S. Irlle, J. H. Warner, H. Kataura and H. Shinohara, *Nat. Commun.*, 2013, **4**, 2548.
- 111 P. Gallay, M. Eguílaz and G. Rivas, *Biosens. Bioelectron.*, 2020, **148**, 111764.
- 112 S. Li, Y. Hou, Q. Chen, X. Zhang, H. Cao and Y. Huang, *ACS Appl. Mater. Interfaces*, 2020, **12**, 2581–2590.
- 113 Y.-P. Sun, B. Zhou, Y. Lin, W. Wang, K. A. S. Fernando, P. Pathak, M. J. Mezziani, B. A. Harruff, X. Wang, H. Wang, P. G. Luo, H. Yang, M. E. Kose, B. Chen, L. M. Veca and S.-Y. Xie, *J. Am. Chem. Soc.*, 2006, **128**, 7756–7757.
- 114 X. Xu, R. Ray, Y. Gu, H. J. Ploehn, L. Gearheart, K. Raker and W. A. Scrivens, *J. Am. Chem. Soc.*, 2004, **126**, 12736–12737.
- 115 S. Y. Lim, W. Shen and Z. Gao, *Chem. Soc. Rev.*, 2015, **44**, 362–381.
- 116 Y. Lv, M. Ma, Y. Huang and Y. Xia, *Chem. – Eur. J.*, 2019, **25**, 954–960.
- 117 A. K. Shukla, C. Sharma and A. Acharya, *ACS Appl. Mater. Interfaces*, 2021, **13**, 15040–15052.
- 118 J. Zhao, H. Wang, H. Geng, Q. Yang, Y. Tong and W. He, *ACS Appl. Nano Mater.*, 2021, **4**, 7253–7263.
- 119 C. Dong, S. Wang, M. Ma, P. Wei, Y. Chen, A. Wu, Z. Zha and H. Bi, *Appl. Mater. Today*, 2021, **25**, 101178.
- 120 S. Iijima, *Nature*, 1991, **354**, 56–58.
- 121 X. Zhu, P. Liu, Y. Ge, R. Wu, T. Xue, Y. Sheng, S.-R. Ai, K. Tang and Y. J. J. O. E. C. Wen, *J. Electroanal. Chem.*, 2020, **862**, 113940.



- 122 Y. Song, X. Wang, C. Zhao, K. Qu, J. Ren and X. Qu, *Chemistry*, 2010, **16**, 3617–3621.
- 123 R. Zhang, N. Lu, J. Zhang, R. Yan, J. Li, L. Wang, N. Wang, M. Lv and M. Zhang, *Biosens. Bioelectron.*, 2020, **150**, 111881.
- 124 H. Peng, J. Zhang, C. Zeng, C. Zhou, Q. Li, N. Lu and L. Wang, *ACS Appl. Bio. Mater.*, 2020, **3**, 5111–5119.
- 125 Y. Yang, T. Li, Y. Qin, L. Zhang and Y. Chen, *Front. Chem.*, 2020, **8**, 564968.
- 126 Y. He, X. Niu, L. Shi, H. Zhao, X. Li, W. Zhang, J. Pan, X. Zhang, Y. Yan and M. Lan, *Microchim. Acta*, 2017, **184**, 2181–2189.
- 127 Y. Li, Y. Lu, X. Zhang, H. Cao and Y. Huang, *ACS Appl. Nano Mater.*, 2021, **4**, 9547–9556.
- 128 M. J. Allen, V. C. Tung and R. B. Kaner, *Chem. Rev.*, 2010, **110**, 132.
- 129 K. M. Tripathi, T. Kim, D. Losic and T. T. Tung, *Carbon*, 2016, **110**, 97–129.
- 130 S. Jung, P. Thi Huong, S. Sahani, K. M. Tripathi, B. J. Park, Y. H. Han and T. Kim, *J. Electrochem. Soc.*, 2022, **169**, 010509.
- 131 T. T. Tung, M. Mouss, K. M. Tripathi, T. Kim, M. J. Nine, A. K. Nanjundan, D. Dubal and D. Losic, *Sustain. Mater. Technol.*, 2022, e00393, DOI: 10.1016/j.susmat.2022.e00393.
- 132 S. Pandit and M. De, *Nanoscale Adv.*, 2021, **3**, 5102–5110.
- 133 Y. Hou, Y. Lu, Q. Chen, X. Zhang and Y. Huang, *Sens. Actuators, B*, 2021, **333**, 129549.
- 134 Y. Zhu, T. Xue, Y. Sheng, J. Xu, X. Zhu, W. Li, X. Lu, L. Rao and Y. Wen, *Microchem. J.*, 2021, **170**, 106697.
- 135 J. Zhang, S. Wu, L. Ma, P. Wu and J. Liu, *Nano Res.*, 2020, **13**, 455–460.
- 136 A. Sun, L. Mu and X. Hu, *ACS Appl. Mater. Interfaces*, 2017, **9**, 12241–12252.
- 137 Y. Wu, J. Wen, W. Xu, J. Huang, L. Jiao, Y. Tang, Y. Chen, H. Yan, S. Cao, L. Zheng, W. Gu, L. Hu, L. Zhang and C. Zhu, *Small*, 2021, **17**, 2101907.
- 138 X. Zhou, M. You, F. Wang, Z. Wang, X. Gao, C. Jing, J. Liu, M. Guo, J. Li, A. Luo, H. Liu, Z. Liu and C. Chen, *Adv. Mater.*, 2021, **33**, 2100556.
- 139 W. Ma, Y. Xue, S. Guo, Y. Jiang, F. Wu, P. Yu and L. Mao, *Chem. Commun.*, 2020, **56**, 5115–5118.
- 140 J. Li, K. Yi, Y. Lei, Z. Qing, Z. Zou, Y. Zhang, H. Sun and R. Yang, *Chem. Commun.*, 2020, **56**, 6285–6288.
- 141 T. Wang, Q. Bai, Z. Zhu, H. Xiao, F. Jiang, F. Du, W. W. Yu, M. Liu and N. Sui, *Chem. Eng. Sci.*, 2021, **413**, 127537.
- 142 X. Gao, H. Liu, D. Wang and J. Zhang, *Chem. Soc. Rev.*, 2019, **48**, 908–936.
- 143 Y. Myung, S. Jung, T. T. Tung, K. M. Tripathi and T. Kim, *ACS Sustainable Chem. Eng.*, 2019, **7**, 3772–3782.
- 144 L. Wang, B. Li, Z. You, A. Wang, X. Chen, G. Song, L. Yang, D. Chen, X. Yu, J. Liu and C. Chen, *Anal. Chem.*, 2021, **93**, 11123–11132.
- 145 Q. Wang, X. Zhang, L. Huang, Z. Zhang and S. Dong, *ACS Appl. Mater. Interfaces*, 2017, **9**, 7465–7471.
- 146 N. Qiu, Y. Liu, M. Xiang, X. Lu, Q. Yang and R. Guo, *Sens. Actuators, B*, 2018, **266**, 86–94.
- 147 X. Cai, H. Chen, Z. Wang, W. Sun, L. Shi, H. Zhao and M. Lan, *Biosens. Bioelectron.*, 2019, **123**, 101–107.
- 148 J. Mou, X. Xu, F. Zhang, J. Xia and Z. Wang, *ACS Appl. Bio Mater.*, 2020, **3**, 664–672.
- 149 N. Qiu, Y. Liu and R. Guo, *ACS Appl. Mater. Interfaces*, 2020, **12**, 15553–15561.
- 150 Y. Zhu, P. Liu, T. Xue, J. Xu, D. Qiu, Y. Sheng, W. Li, X. Lu, Y. Ge and Y. Wen, *Microchem. J.*, 2021, **162**, 105855.
- 151 N. Lu, X. Yan, Y. Gu, T. Zhang, Y. Liu, Y. Song, Z. Xu, Y. Xing, X. Li, Z. Zhang and S. Zhai, *Electrochim. Acta*, 2021, **395**, 139197.
- 152 N. Qiu, Y. Liu and R. Guo, *ACS Appl. Mater. Interfaces*, 2020, **12**, 15553–15561.
- 153 J. Zhang, N. Lu, H. Peng, J. Li, R. Yan, X. Shi, P. Ma, M. Lv, L. Wang, Z. Tang and M. Zhang, *Nanoscale*, 2020, **12**, 5186–5195.
- 154 C. Zhang and X. Du, *Front. Chem.*, 2020, **8**, 651.
- 155 H. Ding, B. Hu, B. Zhang, H. Zhang, X. Yan, G. Nie and M. Liang, *Nano Res.*, 2021, **14**, 570–583.
- 156 K. Habiba, D. P. Bracho-Rincon, J. A. Gonzalez-Feliciano, J. C. Villalobos-Santos, V. I. Makarov, D. Ortiz, J. A. Avalos, C. I. Gonzalez, B. R. Weiner and G. Morell, *Appl. Mater. Today*, 2015, **1**, 80–87.
- 157 M. Swierczewska, K. Y. Choi, E. L. Mertz, X. Huang, F. Zhang, L. Zhu, H. Y. Yoon, J. H. Park, A. Bhirde, S. Lee and X. Chen, *Nano Lett.*, 2012, **12**, 3613–3620.
- 158 R. G. Mahmudunnabi, F. Z. Farhana, N. Kashaninejad, S. H. Firoz, Y.-B. Shim and M. J. A. Shiddiky, *Analyst*, 2020, **145**, 4398–4420.
- 159 Y. Shu, Z. Li, Y. Yang, J. Tan, Z. Liu, Y. Shi, C. Ye and Q. Gao, *ACS Appl. Nano Mater.*, 2021, **4**, 7954–7962.
- 160 K. Wang, C. Wu, F. Wang, M. Liao and G. Jiang, *Biosens. Bioelectron.*, 2020, **150**, 111869.
- 161 L. Su, S. Qin, Y. Cai, L. Wang, W. Dong, G. Mao, S. Feng, Z. Xie and H. Zhang, *Sens. Actuators, B*, 2022, **353**, 131150.
- 162 T. Feng, X. Qiao, H. Wang, Z. Sun, Y. Qi and C. Hong, *J. Mater. Chem. B*, 2016, **4**, 990–996.
- 163 Z. Lou, S. Zhao, Q. Wang and H. Wei, *Anal. Chem.*, 2019, **91**, 15267–15274.
- 164 M. P. Landry, H. Ando, A. Y. Chen, J. Cao, V. I. Kottadiel, L. Chio, D. Yang, J. Dong, T. K. Lu and M. S. Strano, *Nat. Nanotechnol.*, 2017, **12**, 368–377.
- 165 J. Zhang, J. Lei, C. Xu, L. Ding and H. Ju, *Anal. Chem.*, 2010, **82**, 1117–1122.
- 166 H. Ren, L. Yan, M. Liu, Y. Wang, X. Liu, C. Liu, K. Liu, L. Zeng and A. Liu, *Sens. Actuators, B*, 2019, **296**, 126517.
- 167 S. Yousefinejad, H. Rasti, M. Hajebi, M. Kowsari, S. Sadravi and F. Honarasa, *Sens. Actuators, B*, 2017, **247**, 691–696.
- 168 R. Qin, Y. Feng, D. Ding, L. Chen, S. Li, H. Deng, S. Chen, Z. Han, W. Sun and H. Chen, *ACS Appl. Bio Mater.*, 2021, **4**, 5520–5528.
- 169 L. Wang, L. Zhuang, S. He, F. Tian, X. Yang, S. Guan, G. I. N. Waterhouse and S. Zhou, *ACS Appl. Mater. Interfaces*, 2021, **13**, 59649–59661.
- 170 Y. Yang, D. Zhu, Y. Liu, B. Jiang, W. Jiang, X. Yan and K. Fan, *Nanoscale*, 2020, **12**, 13548–13557.



- 171 X. Pan, L. Bai, H. Wang, Q. Wu, H. Wang, S. Liu, B. Xu, X. Shi and H. Liu, *Adv. Mater.*, 2018, **30**, 1800180.
- 172 L. Wu, Q.-S. Guo, Y.-Q. Liu and Q.-J. Sun, *Anal. Chem.*, 2015, **87**, 5318–5323.
- 173 J. Wang, R. Huang, W. Qi, R. Su, B. P. Binks and Z. He, *Appl. Catal., B*, 2019, **254**, 452–462.
- 174 X. Lu, G. Liu, P. Di, Y. Li, T. Xue, X. Duan, Y. Wen, Y. Zhu, Y. Cai, Q. Xu and J. Xu, *Food Anal. Methods*, 2020, **13**, 2028–2038.
- 175 Y. Wang, Y. Wang, F. Wang, H. Chi, G. Zhao, Y. Zhang, T. Li and Q. Wei, *J. Colloid Interface Sci.*, 2022, **606**, 510–517.
- 176 P. K. Boruah and M. R. Das, *J. Hazard. Mater.*, 2020, **385**, 121516.
- 177 J. Wei, Y. Yang, J. Dong, S. Wang and P. Li, *Mikrochim. Acta*, 2019, **186**, 66.
- 178 Y. Mao, S. Gao, L. Yao, L. Wang, H. Qu, Y. Wu, Y. Chen and L. Zheng, *J. Hazard. Mater.*, 2021, **408**, 124898.
- 179 M. Devi, P. Das, P. K. Boruah, M. J. Deka, R. Duarah, A. Gogoi, D. Neog, H. S. Dutta and M. R. Das, *J. Environ. Chem. Eng.*, 2021, **9**, 104803.
- 180 Z. Mohammadpour, A. Safavi and M. Shamsipur, *Chem. Eng. J.*, 2014, **255**, 1–7.
- 181 S. Chandra, V. K. Singh, P. K. Yadav, D. Bano, V. Kumar, V. K. Pandey, M. Talat and S. H. Hasan, *Anal. Chim. Acta*, 2019, **1054**, 145–156.
- 182 Q. Li, D. Yu, C. Fan, Q. Huang, Y. Tang, R. Guo, Y. Huang, H. Wang, C. Lin and Y. Lin, *ACS Appl. Nano Mater.*, 2022, **5**, 94–100.
- 183 P. Borthakur, P. K. Boruah and M. R. Das, *ACS Sustainable Chem. Eng.*, 2021, **9**, 13245–13255.
- 184 P. Borthakur, P. K. Boruah and M. R. Das, *J. Environ. Chem. Eng.*, 2021, **9**, 104635.

